Energetics and Vertical Structure of the Thermohaline Circulation

David Sproson
Supervised by Prof. D. Marshall

Department of Mathematics
University of Reading
August 2005

Abstract

There has long been a misconception that the oceanic thermohaline circulation is driven by buoyancy forcing at the ocean surface. However, energy arguments dating as far back as Sandström (1908) show that a fluid heated and cooled at the surface cannot maintain an overturning circulation more substantial than a circulation limited by molecular diffusion. Mechanical forcing is thus required to sustain the observed circulation by vertically mixing dense abyssal fluid with lighter fluid above, supplying potential energy to the ocean. Once this is established, questions of which processes drive the oceanic mixing arise.

This study first reviews the work to date on the energetics of the general circulation, following it through to the suprising conclusion that tides, particularly the semi-diurnal lunar tide, provide much of the energy to the general circulation.

The consideration of vertical mixing leads to an examination of the vertical structure and equilibria in the thermohaline circulation through a series of simple analytic models. The behaviour of a two layer model proposed by Gnanadesikan (1999) is investigated and it is found that the model does not support multiple equilibria seen in many other models, notably in a two box model proposed by Stömmel (1961). An attempt is made to reconcile these two models through a reparameterisation of a process in Gnanadesikan's two layer model, which forces the existence of multiple equilibria. While successful, further work is required to place this parameterisation on a rigorous footing.

Declaration

I confirm that this is my own work, and the use of all material from other sources has been properly and fully acknowledged.

David Sproson.

Acknowledgements

I would like to thank my supervisor, David Marshall, for all of his help and support over the last few months, for many interesting discussions and for suggesting an interesting topic in the first place.

Thanks also to my housemates for distracting me at all the right times and then leaving the country when I really had to get on with some work, and to all of the folk from maths and meteorology for making the year so enjoyable.

Finally, I would like to thank my family for their ongoing love and support.

I would like to acknowledge the financial support received from the Natural Environment Research Council.

Symbols, Abbreviations and Acronyms

α - Thermal expansion coeffecient

β - Saline expansion coefficient or meridional derivative of the Coriolis frequency

ϵ - Energy dissipation per unit mass

Γ - Mixing efficiency

κ - Diffusivity

μ - Dynamic coefficient of viscosity

ν - Molecular coefficient of viscosity

ρ - Density

τ - Surface wind stress. In vector form this is the 3-D wind stress vector consisting of components τ_x, τ_y, τ_z. In scalar form it is the zonal wind stress

A - Area of the low latitude oceans over which upwelling occurs

A_i - Southern Ocean eddy diffusivity

c_d - Ocean bottom drag coefficient

D - Pycnocline depth

E - Freshwater transport

f - Coriolis frequency

K - Turbulent diffusivity

K_v - Vertical turbulent diffusivity

L_x - Circumference of the Earth at Drake Passage latitudes

L_y^n - Distance over which the pycnocline rises D to 0 in the north

L_y^s - Distance over which the pycnocline rises D to 0 in the south

p - Pressure

q - Volume Transport

Q_n - Northern hemisphere sinking

Q_s - Southern Ocean upwelling

Q_u - Low latitude upwelling

S - Salinity in parts per thousand

T - Temperature

THC - Thermohaline circulation

$\mathbf{u}$ - 3-D velocity vector consisting of components u, v, w

Contents

List of Figures

Chapter 1

Introduction

1.1 The Thermohaline Circulation

There is presently a great interest in the area of the Earth's climate, and how it has changed in the past and will change in the future in response to both natural and man-made forcing. Many of the ideas of climate change, and particularly rapid climate change, rely on variability in the oceanic thermohaline circulation. Many theories of rapid climate change rely on such a circulation supporting multiple equilibria. However, there has long been confusion and discrepancies in the literature about what the thermohaline circulation is, and perhaps more fundamentally about where the energy which drives the circulation arises.

Why is there so much interest in the thermohaline circulation? The thermohaline circulation is capable of transporting a huge amount (upto 2 PW) of heat from the tropics to polar regions, and is in no small way responsible for the temperate climate in certain areas of the northern hemisphere. However, it is believed that the thermohaline circulation may have more than one, possibly many, stable equilibrium states. It is also believed that even a relatively modest change to the freshwater transport in the North Atlantic could cause the thermohaline circulation here to jump to another stable mode, for example where the buoyancy controlled sinking the the North Atlantic is replaced by a much slower salt driven upwelling, a mode similar to that found in the current day North Pacific. Such a circulation would provide little or no heat to the North Atlantic, and would have far reaching consequences on the future climate. While the circulation time of the thermohaline circulation is a few millennia, a change between two stable

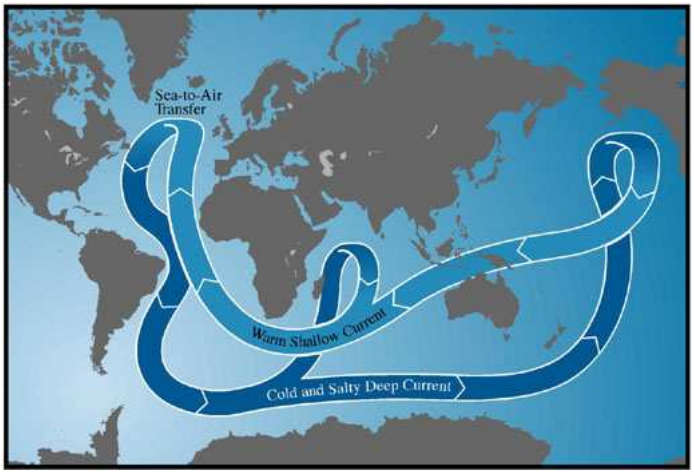

Figure 1.1: A highly simplified schematic of the thermohaline circulation. This conveyor belt visualization of the thermohaline circulation was put forward by W.S. Broecker in 1987. While this gives an adequate overview of the thermohaline circulation, it neglects the Ekman driven upwelling in the Southern Ocean which is of great importance to this study. Source: `http://www.grico.org`

modes could occur on a decadal timescale.

In this report we choose to sidestep the precise definition of what constitutes the thermohaline circulation; for a discussion on how best to define the thermohaline circulation see Wunsch & Ferrarri (2002). We will consider the thermohaline circulation to be a kind of meridional overturning circulation capable of exporting huge amounts of heat and salt from the low latitudes to polar regions and concentrate on where the energy to drive such a circulation arises and the impact of these energy sources on the strength and vertical structure of the circulation.

1.2 Sandström's Theorem

In the early 1900's, Sandström conducted a series of laboratory experiments in which fluids were heated and cooled at different levels, and analysed the results in terms of an idealized heat engine. He considered three cases: 1. heating at a higher pressure than cooling, 2. heating at a lower pressure than cooling, 3. heating and cooling at the same pressure. It was shown that in the first case the circulation was strong and controlled by friction - work could be extracted from the fluid as expansion was taking place at a higher pressure than was contraction.

In the second case the fluid between the heat source and sink became stably stratified, with the fluid below the sink becoming homogeneous at the temperature of the sink. The only flow in the fluid was a very weak diffusion limited motion between the source and sink. When the source and sink were located at the same level (but laterally separated) a weak overturning flow was observed between the two plates.

These observations led Sandström to the following conclusion, now usually referred as Sandström's Theorem: "A closed steady circulation can be maintained in the ocean only if the heating source is located at a lower level than the cooling source."

In the ocean, most of the heating and cooling occurs at the surface, although some heating can penetrate to depths of around 100 metres. This would lead us to believe that the oceanic general circulation consists of a weak thermal current in the upper few hundred metres of the ocean, limited by viscous friction, with a stably stratified and approximately stationary pool of fluid in the abyss. The fact that this in not what is observed in the oceans has brought many people to question the validity of Sandström's theorem in the oceanic case. However, the discrepancies may be explained by the multitude of forcings and processes in the ocean that were not, nor could be, present in Sandström's laboratory experiments.

1.3 Outline of this Study

This study seeks to address questions relating to the energetics of the thermohaline circulation, through a consideration of the global ocean energy budgets, and to consider how the pathways and processes by which energy is transferred to the oceans affects the vertical structure of the thermohaline circulation. Of particular interest is the structure and circulation that would exist under substantially different regimes of energy input, especially under possible climate change scenarios.

In Chapter 2 the energetics of the global ocean, which imply a need for mechanical energy to provide the vertical mixing required to sustain the circulation, are examined. Such mechanical energy can only come from a limited number of sources, which are identified. Each of these sources is then examined to find

which processes are dominant in supplying energy to the oceans.

Having identified the processes most important for providing energy to the thermohaline circulation, in Chapter 3 some original calculations are presented using a simple model of the thermohaline circulation which incorporates these processes. The nature of the circulation and depth of the pycnocline are investigated under various parameter regimes. Chapter 4 examines multiple equilibria in the thermohaline circulation and addresses the paradox of multiple equilibria in a mechanically driven ocean when traditional ideas of multiple equilibria rely on opposing thermal and haline forcing.

Finally in Chapter 5, a summary of the study is given, the key points are discussed and directions for future work are suggested.

Chapter 2

Energetics of the General Circulation

2.1 The Requirement for Mixing Energy

As water in the north Atlantic moves poleward it becomes dense, mainly through exchanges with the atmosphere, and is rendered convectively unstable. Continual sinking of this dense water lowers the potential energy of the ocean system. Without some process returning this dense fluid to the surface, it would gradually fill the oceanic abyss – if abyssal water is produced at a rate of 30 Sv[1] (1 Sv $\equiv 10^6$ m^3s^{-1}), this would happen on a timescale of approximately 3000 years.

Can surface convection produce an interior turbulence capable of re-raising this dense fluid through the stratification? We consider the case of horizontal surface convection, following Paparella & Young (2002). Introducing energy dissipation per unit mass,

$$\epsilon = \nu||\nabla \mathbf{u}||^2 = \frac{\mu}{\rho}\left[\left(\frac{\partial \mathbf{u}}{\partial x}\right)\cdot\left(\frac{\partial \mathbf{u}}{\partial x}\right) + \left(\frac{\partial \mathbf{u}}{\partial y}\right)\cdot\left(\frac{\partial \mathbf{u}}{\partial y}\right) + \left(\frac{\partial \mathbf{u}}{\partial z}\right)\cdot\left(\frac{\partial \mathbf{u}}{\partial z}\right)\right],$$

it is said that a flow cannot be turbulent if ϵ is zero in the limit $R \to \infty$, where R is the Rayleigh or Reynolds number. This can be thought of as being equivalent to the stipulation that any mixing in the fluid occurs purely through diffusion with no input from turbulent processes. It is consistent with *the law of finite energy*

[1]The range of estimates of bottom water production is quite large, however many estimates favour a value of approximately 25-30 Sv.

dissipation: If, in an experiment on turbulent flow, all of the control parameters are kept the same, except for viscosity, ν, which is lowered as much as possible, the energy dissipation per unit mass behaves in a way consistent with a finite positive limit.

Consider a three dimensional rotating fluid, with Coriolis frequency f, in a cuboid domain. The vertical extent of the domain is denoted H, with $-H < z < 0$. No heat flux is permitted through the sides or bottom of the domain. Using the Boussinesq approximation, the equations of motion for this fluid are

$$\left.\begin{array}{c} \frac{D\mathbf{u}}{Dt} + f\hat{\mathbf{k}} \times \mathbf{u} + \nabla p = b\hat{\mathbf{k}} + \nu\nabla^2\mathbf{u}, \\ \frac{Db}{Dt} = \kappa\nabla^2 b, \\ \nabla \cdot \mathbf{u} = 0, \end{array}\right\} \tag{2.1}$$

where $b = g\alpha\,(T - T_0)$ is the buoyancy, p the pressure, ν the kinematic viscosity, κ the thermal diffusivity and $\mathbf{u} = (u, v, w)$ the velocity. The density, ρ, is given by $\rho = \rho_0\,(1 - b/g)$. It is assumed that $\mathbf{u}\cdot\hat{\mathbf{n}} = 0$ and that there is 'some combination' of no slip and no stress boundary conditions. The surface buoyancy, $b\,(x, y, 0, t)$, which should be non-constant at least in space, is prescribed.

Denoting by an overbar spatial and, where necessary to assume a steady field, temporal averages, we have from (2.1), the no flux boundary condition and the fact that $\bar{b} = \bar{b}(z)$, that

$$\overline{wb} - \kappa\bar{b}_z = 0, \tag{2.2}$$

i.e. there is, on average, no vertical buoyancy flux through any level $z =$ constant.

Let us denote the average of a field over the domain by angular brackets,

$$\langle\theta\rangle = \frac{1}{V}\int_V \theta\,(x, y, z, t)\ \mathrm{d}V = \frac{1}{H}\int_{-H}^{0} \bar{\theta}\,(z)\ \mathrm{d}z.$$

Taking the scalar product of $\mathbf{u}$ with the momentum equation in (2.1) and averaging over the domain, we obtain

$$\epsilon \equiv \nu||\nabla\mathbf{u}||^2 = \langle wb\rangle. \tag{2.3}$$

Averaging (2.2) over z, we obtain

$$\langle wb\rangle = \frac{\kappa}{H}\left[\bar{b}(0) - \bar{b}(-H)\right]$$

and hence

$$\nu||\nabla \mathbf{u}|| = \frac{\kappa}{H}\left[\bar{b}(0) - \bar{b}(-H)\right]. \tag{2.4}$$

It has been shown, for example Protter and Weinberger (1984), that the buoyancy in the domain must be bounded above and below by the maximum and minimum buoyancy values imposed at the surface. This being the case, we have

$$\bar{b}(0) - \bar{b}(-H) < b_{\max} - b_{\min}$$

and thus

$$\epsilon \equiv \nu||\nabla \mathbf{u}||^2 < \frac{\kappa}{H}\left(b_{\max} - b_{\min}\right). \tag{2.5}$$

Taking the diffusivity to the limit $\kappa \to 0$, with ν/κ fixed, we see that $\epsilon \to 0$; surface buoyancy forcing in the ocean cannot generate an interior turbulence to re-raise the dense fluid, as one would expect from Sandström's theorem. In fact, this anti-turbulence theorem can be thought of as putting Sandström's theorem on a rigorous footing.

In view of Sandström's theorem and the above result, it must be conceded that there are other processes at work on the ocean supplying mixing energy, allowing dense fluid to return to the surface. However, exactly how and where this happens is still not clearly known. Munk (1966) assumed a uniform upwelling throughout the entire deep ocean. He considered a simple one-dimensional balance between advection and diffusion

$$w\frac{\partial \rho}{\partial z} = \kappa \frac{\partial^2 \rho}{\partial z^2} \tag{2.6}$$

where w, κ were assumed everywhere constant. This was justified from density sections such as Figure 2.1 where, in the abyss and away from the Southern Ocean upwelling, the isopycnals are approximately horizontal. When fitted to observed profiles in the Pacific, Munk found values of $w \approx 0.7 \times 10^{-7}$ ms^{-1}, $\kappa \approx 10^{-4}$ m^{2}s^{-1}. The value of w here was calculated from an estimated bottom water production, Q, of 25 Sv.

Munk's study left us requiring a vertical diffusivity[2] of $K \approx 10^{-4}$ m^{2}s^{-1} to sustain the oceanic circulation, with an associated energy source supplying the work required to raise the fluid across the stratification. In subsequent years a

[2]We use K rather than κ here as the required mixing rate implied by Munk's study is much larger than the molecular diffusivity of temperature or salt, and so this must represent a turbulent rather than diffusive process.

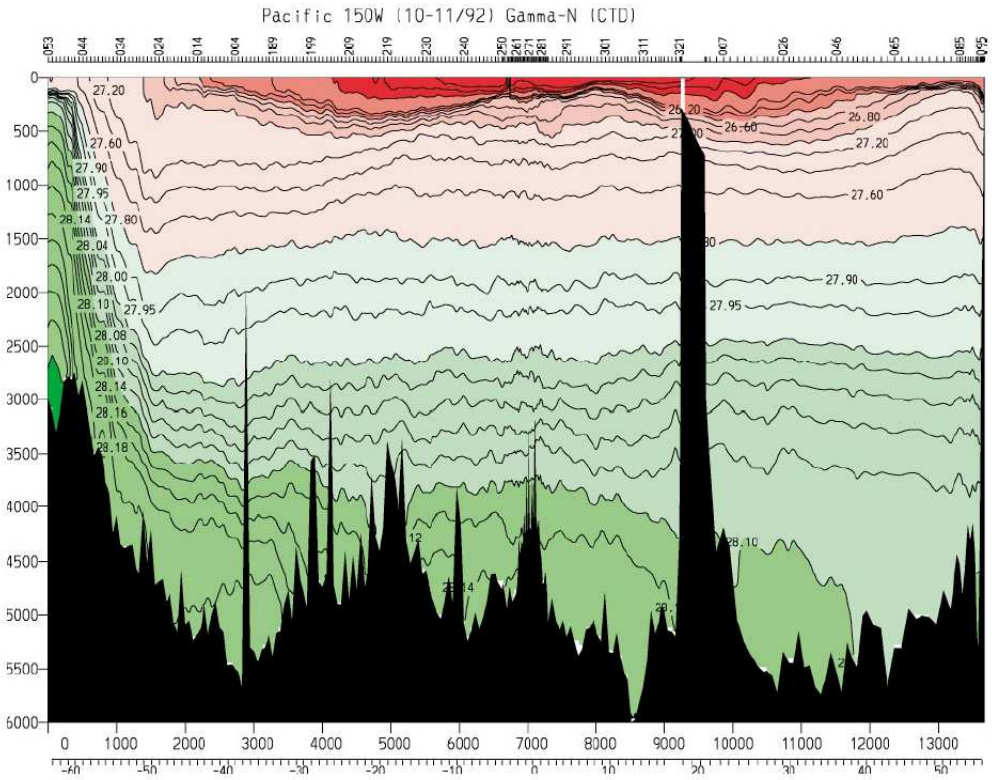

Figure 2.1: Meridional neutral density section in the central Pacific Ocean, from Wunsch & Ferrari (2004). Notice that below the pycnocline (at approximately 700 m) and away from the Southern Ocean upwelling the isopycnals are approximately horizontal. This led Munk (1966) to introduce a one-dimensional balance between advection and diffusion as a process for maintaining the stratification.

Ocean/Depth	$\langle K \rangle (10^{-4} \mathrm{m^2 s^{-1}})$	Reference
Atlantic, bottom	9 ± 4	Ganachaud & Wunsch (2000)
Indian, bottom	12 ± 7	Ganachaud & Wunsch (2000)
Pacific, bottom	9 ± 2	Ganachaud & Wunsch (2000)
Atlantic, deep	3 ± 1.5	Ganachaud & Wunsch (2000)
Indian, deep	4 ± 2	Ganachaud & Wunsch (2000)
Pacific, deep	4 ± 1	Ganachaud & Wunsch (2000)
Scotia Sea	30 ± 10	Ganachaud & Wunsch (2000)
Brazil Basin	3.5 ± 0.5	Heywood et al. (2002)
Samoan Passage	500	Roemmich et al. (1996)
Amirante Trench	10.6 ± 2.7	Barton & Hill (1989)
Discovery Gap	1.5–4	Saunders (1987)
Romanche Fracture Zone	100	Ferron et al. (1998)

Table 2.1: Averaged diapycnal mixing rates in various locations. Adapted from Wunsch & Ferrari (2004).

number of observational campaigns were carried out to attempt to measure the rate at which vertical mixing occurs. The wide range of results obtained only serve to complicate the situation.

2.2 Observations and Measurements

The first direct estimates of vertical mixing in the oceans were not made until the early 1980s. Hogg et al. (1982) estimated the vertical mixing in the Brazil Basin by determining the flux of dense fluid entering the basin. Antarctic bottom water (AABW) enters the Brazil Basin through deep water inlets – the Vema and Hunter Channels – and moves north. Such dense water (AABW generally has a potential temperature, θ, of less than 2 °C) cannot escape through the channel at 36° W nor through the Romanche or Chain Fracture Zones and so must be mixing vertically if the Brazil Basin is to maintain a constant volume.

Using the steady state heat balance

$$\int_V \nabla \cdot (\mathbf{u}\theta) \, \mathrm{d}V = \int_V (\kappa \theta_z)_z \, \mathrm{d}V, \tag{2.7}$$

where V is the volume bounded above by an isothermal surface and below by the

sea floor, and rewriting this as

$$\int_A \mathbf{u}\theta \cdot \hat{\mathbf{n}} \, \mathrm{d}A = \left[\overline{\kappa\theta}_z A\right]_{\text{top}} - \left[\overline{\kappa\theta}_z A\right]_{\text{bottom}} \tag{2.8}$$

where A is the area of V normal to $\hat{\mathbf{n}}$, Hogg was able to imply a vertical (diapycnal) diffusivity $\kappa = 3.5 \pm 0.5 \times 10^{-4}$ m^{2}s^{-1} by assuming $\overline{\kappa\theta_z} = \overline{\kappa}\overline{\theta}_z$.

Using the same or similar methods, numerous other estimates of vertical mixing were produced, with most lying around the Munk (1966) value of 10^{-4} m^{2}s^{-1}. Over areas of complex bottom topography, and particularly around deep channels (e.g. The Romanche Fracture Zone), however, considerably larger mixing rates were implied.

It was noted by Cox and others that any turbulent processes which cause the mixing must be dissipated, and eventually this must happen on the molecular level, so dissipation must be dependent on the molecular diffusivities for temperature and salt, κ_T & κ_S respectively. Osborn and Cox (1972) showed, under a number of simplifying assumptions[3], that

$$3\kappa_T \overline{\left(\frac{\partial T'}{\partial z}\right)^2} = K \left(\frac{\partial \overline{T}}{\partial z}\right)^2,$$

where the overbar is a spatial average over $O(10)$ metres and the prime indicates a deviation from it. Enough small scale structure $(\partial T'/\partial z)^2$ must be present to allow dissipation of the turbulent kinetic energy. The development of profiling devices which could measure temperature and velocity to scales of 10^{-3} m allowed K to be measured directly. Later, work by Osborn (1980) allowed inference of mixing from viscous dissipation, ϵ, which could now also be measured by velocity profiling instruments. Most of the turbulent kinetic energy in the ocean is dissipated through viscous friction, however the remaining fraction, Γ, is available to vertically mix the fluid, with $\Gamma\epsilon = KN^2$ Wkg^{-1}. The problem with this approach is that Γ is poorly quantified. It is generally thought to be around 0.2; however its spatial variability is unknown.

The results of both of these approaches of measuring K were generally in disagreement with the observational campaigns, both failing to produce mixing

[3]notably neglecting thermal advection; this model is inappropriate in areas of large temperature gradients.

rates in the open ocean of more than $O(10^{-5})$ m^{2}s^{-1}, around a tenth of the value observations required to support the general circulation.

More recently, e.g. Ledwell et al (1998, 2000), a series of tracer release experiments have been conducted, tracking a dye which was injected into the ocean at depth. The results only went to confirm the value of $K = O(10^{-5})$ m^{2}s^{-1} in the open ocean. Similar experiments, primarily conducted in lakes with dye released near the boundaries suggested that mixing may well be enhanced where fluid interacts with topography, however the results were poorly quantified and no values for mixing rates at the boundary were given.

With advances in technology it became possible to directly measure the small scale structure of the ocean all the way to the sea floor. It was found that mixing rates of $K \approx O(10^{-5})$ m^{2}s^{-1} exist all the way to the bottom over abyssal plains and other simple structures. Over more complicated structures such as the mid-ocean ridges and deep canyons, however, mixing rates were much enhanced and had a tendency to increase with depth. This increased mixing over complex three-dimensional topography is probably due to the breaking of the internal wave field as tidal processes and the general circulation force fluid over the relief.

It seems, then, that the vast majority of ocean mixing occurs at the boundary. However, observations have not described any significant variations in temperature/salinity characteristics between the ocean interior and the boundary where these characteristics are obtained; they must thus be readily transported from the boundary to the interior, presumably along neutral surfaces. Munk & Wunsch (1998) explored an extension of Munk's one-dimensional model (2.6), allowing for lateral homogenisation by including a horizontal advection term:

$$\kappa_{\rm PE}\frac{\partial^2\rho}{\partial z^2} - w\frac{\partial\rho}{\partial z} - u\frac{\partial\rho}{\partial x} = 0, \tag{2.9}$$

where $\kappa_{\rm PE}$, the so called 'pelagic dissipation' is the vertical diffusivity in the open ocean, typically 10^{-5} m^{2}s^{-1}. At $x = 0$, the lateral boundary, the density distribution $\rho(0, z)$ was taken to be characteristic of $\kappa = 10^{-4}$ m^{2}s^{-1}. The density profile at infinity, $\rho(\infty, z)$ was taken to be characteristic of $\kappa_{\rm PE}$, which is approached for large positive x. There is a question here of whether 10^{-4} m^{2}s^{-1} is a large enough mixing rate to take at the boundary, as boundary mixing would have to be significantly higher to account for the global average of 10^{-4} m^{2}s^{-1}. To simplify the solution, the region of intense boundary mixing was, somewhat

un-physically, confined to $x < 0$. The solution is omitted here (however see Munk & Wunsch (1998), Appendix B). Where $u = 0$, (2.9) is reduced to the Munk (1966) balance between vertical advection and diffusion, which has a scale depth of approximately 100 m associated with diffusivity $\kappa_{\rm PE}$ over the entire ocean basin. As $u \to \infty$, the basin average diffusivity tends to the boundary value of $\kappa = 10^{-4}$ m^{2}s^{-1} giving a scale depth of 1 km. Assuming a typical basin width of 10000 km, it was shown that the solution approached the $u = 0$ case for $u \leq O(0.1)$ mms^{-1} and the $u \to \infty$ case for $u \geq O(1)$ mms^{-1}. Typical mesoscale circulation rates in the ocean are usually well above the 1 mms^{-1} required for the solution to approximate the $u \to \infty$ case. The upshot of this is that it seems that horizontal advection is capable of transporting T,S characteristics into the ocean interior. Of course, this model is far from realistic, not only in its lack of dimensionality but also in its treatment of u as a constant everywhere in the domain, which is clearly not the case in reality. However, despite these shortcomings, the model may provide an adequate description of the process by which lateral homogenisation occurs.

Marotzke (1997) considered the effects of boundary processes on a full ocean general circulation model (GCM) forced simply by a tendency to restore temperature and salinity at the surface on a timescale of 30 days. Wind stress and other forcings were neglected. Marotzke, in fact, took his investigation to the limit of zero vertical diffusivity in the interior, arguing that an increase in vertical diffusivity leads to enhanced numerical stability so his method could trivially be extended to the case of non-zero vertical diffusivity. It is worth noting a major shortcoming in this method – that diapycnal mixing in the interior was not totally eradicated due to horizontal advection of fluid across sloping isopycnals. Marotzke compared the circulations between the boundary mixing and uniform mixing cases, with the ocean integrated mixing equal in each case. The results were qualitatively similar, however the uniform mixing case had an overturning rate 18% weaker and a meridional heat transport some 25% weaker than when all mixing was occurring at the boundary, Figure 2.2. Mixing rates in each case are given in the caption. In the boundary mixing case, the meridional heat transport obeys a power law remarkably precisely, with transport $\propto K^{2/3}$.

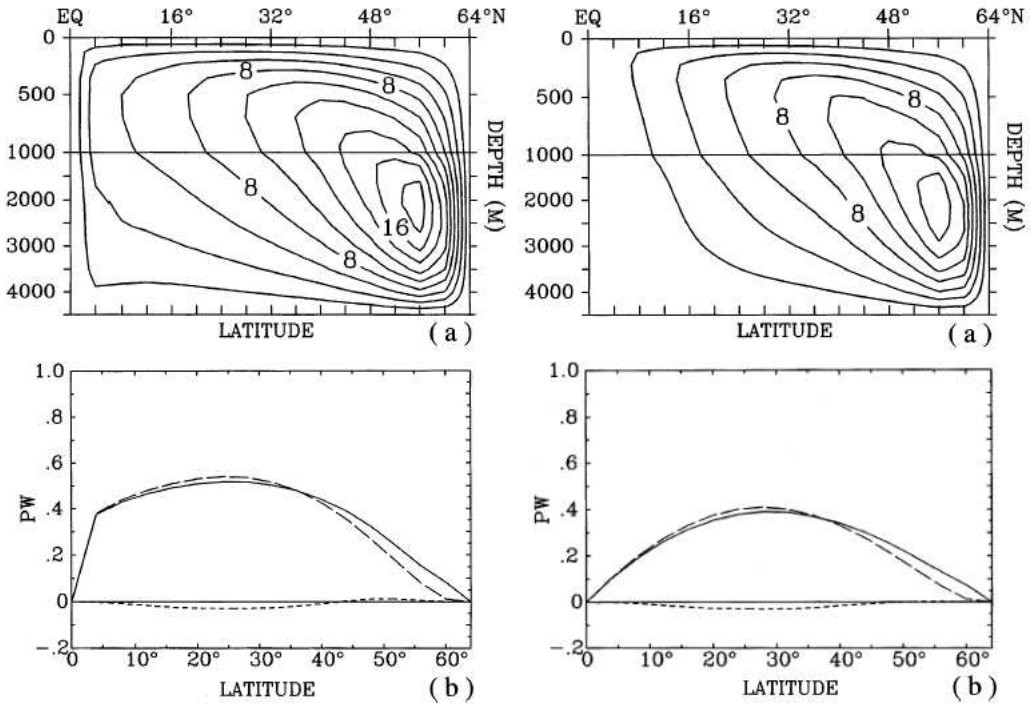

Figure 2.2: Comparing the meridional overturning circulation (a) and meridional heat transport (b) for boundary mixing (left) and uniform mixing (right) cases in a low resolution global circulation model. For the boundary mixing case the vertical diffusivity, $K = 5 \times 10^{-4}$ m^{2}s^{-1} and for the uniform mixing case $K = 0.9 \times 10^{-4}$ m^{2}s^{-1}. In each case in (b) the solid line is the total heat transport, the long dashed line the overturning contribution and the short dashed line the gyre contribution. Adapted from Marotzke (1997).

2.3 Global Ocean Energy Budgets

2.3.1 How much energy is required to support the circulation?

If we assume that the energy required to sustain the circulation is balanced by the turbulent dissipation we can arrive at a figure for the energy input required. The global turbulent dissipation, D, is given by vertically integrating ϵ and multiplying by the area of the global ocean, A.

$$D = A \int \rho\epsilon \, \mathrm{d}z = A\rho\Gamma^{-1}K \int N^2 \, \mathrm{d}z = g\Gamma^{-1}KA\Delta\rho \text{ W}.$$

Using standard values $\Gamma = 0.2$, $K = 10^{-4}$ m^{2}s^{-1}, $A = 3.6 \times 10^{14}$ m^2, $\rho = 1000$ kgm^{-3}, $\Delta\rho = 10^{-3}\rho$, this gives a global turbulent dissipation of a little under 2 TW, which will serve as a crude estimate of the input required to support the general circulation. Other, more in-depth studies have been carried out in an attempt to quantify the energy required to maintain the oceanic stratification. For example, Munk & Wunsch (1998) analyzed the Levitus climatology, arriving at a figure of 2.1 TW of mixing energy required to maintain the stratification against 30 Sv of North Atlantic Deep Water formation.

Having identified the need for mixing energy to support the global circulation, and having arrived at an approximate figure for the energy required, we now examine potential sources of energy to see how the required mixing energy is supplied, following Wunsch & Ferrari (2004).

2.3.2 Ocean Energy Equations and Budgets

From the Navier-Stokes equations, we can arrive at the kinetic energy balance for a fixed fluid parcel by taking the scalar product of the momentum equation with $\mathbf{u}$:

$$\frac{\partial}{\partial t}(\rho E) + \nabla \cdot [(p + \rho E)\,\mathbf{u} - \mu \nabla E] = -\rho \mathbf{u} \cdot \nabla\Phi + p\nabla \cdot \mathbf{u} - \rho\epsilon. \tag{2.10}$$

Here, $E = \frac{1}{2}\mathbf{u} \cdot \mathbf{u}$ is the kinetic energy, ρ the local density and μ the dynamic viscosity. The potential Φ, for reasons we will discover, includes the potential supplied by the Earth/Sun/Moon system as well as the Earth's geopotential.

The former will be denoted Φ_{tide}. The internal energy balance for the same fluid parcel is

$$\frac{\partial}{\partial t}(\rho I) + \nabla \cdot \left[\rho I \mathbf{u} + \mathbf{F}_{\text{rad}} - \rho c_p \kappa_T \nabla T - \frac{\partial h_E}{\partial S} \rho \kappa_S \nabla S \right] = -p \nabla \cdot \mathbf{u} + \rho \epsilon, \quad (2.11)$$

where I is the internal energy and $\mathbf{F}_{\text{rad}}$ represents any radiative flux between the atmosphere and ocean, where a flux from the atmosphere to the ocean is positive, which occurs near the surface. The $\rho c_p \kappa_T \nabla T$ term simply represents the irreversible diffusion of heat, with c_p the specific heat of sea water at constant pressure. The final gradient term on the left hand side, $(\partial h_E/\partial S)\rho \kappa_S \nabla S$, is the salinity diffusion term. This represents the generation of heat in the fluid due to solution energy of salt, with $h_E = I + \rho/p$. Note that there are two terms which occur on the right hand side of both (2.10) and (2.11) with opposite sign. These are the routes of conversion between kinetic and internal energy. The $p \nabla \cdot \mathbf{u}$ term, known as the 'compressive work' is the main, reversible route of conversion between kinetic and potential energy, while $\rho\epsilon$ represents the generation of heat through the viscous dissipation of kinetic energy (i.e. friction).

The potential energy balance is given by

$$\frac{\partial}{\partial t}(\rho \Phi) + \nabla \cdot (\rho \Phi \mathbf{u}) = \rho \mathbf{u} \cdot \nabla \Phi + \rho \frac{\partial \Phi_{\text{tide}}}{\partial t}, \quad (2.12)$$

where Φ is as before. The $\rho \mathbf{u} \cdot \nabla \Phi$ term is also present in (2.10), but with an opposite sign. This represents a reversible path between kinetic and potential energy – the route which must be taken for turbulent mixing to maintain the oceanic stratification and permit the existance of the thermohaline circulation.

The equations (2.10) – (2.12) can be converted to global energy budgets by integrating over the global ocean and applying Stokes' Theorem. This gives

$$\begin{aligned} \frac{\partial}{\partial t} \iiint_V \rho E \, \mathrm{d}V = &- \iint_A \rho E \, (\mathbf{u} - \mathbf{u}_s) \cdot \hat{\mathbf{n}} \, \mathrm{d}A - \iint_A (p\mathbf{u} + \mu \nabla E) \cdot \hat{\mathbf{n}} \, \mathrm{d}A \\ &- \mathcal{P} + \mathcal{C} - \mathcal{D}, \end{aligned} \quad (2.13)$$

$$\frac{\partial}{\partial t}\iiint_V \rho I \, \mathrm{d}V = -\iint_A \rho I \, (\mathbf{u} - \mathbf{u}_s) \cdot \hat{\mathbf{n}} \, \mathrm{d}A \\ - \iint_A \left(\mathbf{F}_{\mathrm{rad}} - \rho c_p \kappa_T \nabla T - \frac{\partial h_E}{\partial S} \rho \kappa_S \nabla S \right) \cdot \hat{\mathbf{n}} \, \mathrm{d}A - \mathcal{C} + \mathcal{D}, \tag{2.14}$$

$$\frac{\partial}{\partial t}\iiint_V \rho \Phi \, \mathrm{d}V = -\iint_A \rho \Phi \, (\mathbf{u} - \mathbf{u}_s) \cdot \hat{\mathbf{n}} \, \mathrm{d}A + \iiint_V \rho \frac{\partial \Phi_{\mathrm{tide}}}{\partial t} \, \mathrm{d}V + \mathcal{P} \tag{2.15}$$

where $\mathbf{u}_s$ is the free surface velocity. The script characters $\mathcal{P}$, $\mathcal{C}$ and $\mathcal{D}$ are the volume integrals of the conversion terms in (2.10)–(2.12) and so are energy transformations rather than sources,

$$\mathcal{P} = \iiint_V \rho \mathbf{u} \cdot \nabla \Phi \, \mathrm{d}V, \quad \mathcal{C} = \iiint_V p \nabla \cdot \mathbf{u} \, \mathrm{d}V, \quad \mathcal{D} = \iiint_V \rho \epsilon \, \mathrm{d}V.$$

The first term on the right hand side of each of the equations (2.13)–(2.15) represents advection through the free surface. Making the fairly safe assumption that the ocean is in an approximate steady state, we must have that $\iint_A (\mathbf{u} - \mathbf{u}_s) \approx 0$. Therefore, for any energy to be advected across the surface there must be a correlation between E, Φ, I and the direction of flow of energy (i.e. whether the flow is into or out of the ocean). The second term represents a forcing: surface momentum forcing in (2.13), tidal forcing in (2.14) and buoyancy forcing (including geothermal effects) (in 2.15).

Most of the energy sources and sinks occur at the boundary. However much of the energy generated here does not penetrate into the deep ocean. For example, the wind does a vast amount of work on the ocean, however much of this simply goes into the generation of surface waves and surface turbulence which remains in the surface mixed layer. We are interested in that energy which can penetrate into the interior of the ocean to drive the abyssal mixing.

2.3.3 Abyssal Energy Budgets

In a steady state, taking an average over a sufficiently long time period, the production of kinetic energy in a volume confined by two level surfaces z_1, z_2 and

lateral side boundaries can be written as

$$\iint_A \mathrm{d}A \left[\overline{\rho E w + p w}\right]_{z_1}^{z_2} = -\iiint_V \mathrm{d}V \overline{\rho g w - p \nabla \cdot \mathbf{u} + \rho \mathbf{u} \cdot \nabla \Phi_{\mathrm{tide}} + \rho \epsilon}, \quad (2.16)$$

where an overbar represents a time average. The viscous stresses at the lateral boundaries, $\mu \nabla E \cdot \hat{\mathbf{n}}$, are assumed negligible. We now try to simplify this expression to find the dominant balance in the abyss.

In a steady state, there can be no net mass flux across horizontal surfaces on a long time average, thus

$$\iiint_V \mathrm{d}V \overline{\rho g w} = 0. \quad (2.17)$$

Consider the equation of continuity in the form

$$\frac{\partial \rho}{\partial t} + \nabla \cdot (\rho \mathbf{u}) = 0. \quad (2.18)$$

We can re-write (2.18) as

$$\rho \nabla \cdot \mathbf{u} + \mathbf{u} \cdot \nabla \rho = -\frac{\partial \rho}{\partial t}$$

and hence

$$p \nabla \cdot \mathbf{u} = \frac{-p}{\rho} \frac{D\rho}{Dt}. \quad (2.19)$$

The compressive work is thus proportional to the rate of change in density of a fluid parcel. The density change due to pressure variations on a parcel will be very small due to the ralative imcompressibility of sea-water. The only other way density can be changed is through diffusive heat or salt fluxes, which are also small in the abyssal ocean. The compressive work term can thus be safely neglected in the abyss. This term only becomes significant near the surface, where heat and salt exchanges with the atmosphere can be relatively large.

So (2.17) has now been simplified to

$$\iint_A \mathrm{d}A \left[\overline{\rho E w + \rho w}\right]_{z_1}^{z_2} + \iiint_V \mathrm{d}V \overline{\mathbf{u} \cdot \nabla \Phi_{\mathrm{tide}}} \approx \iiint_V \mathrm{d}V \overline{\rho \epsilon}, \quad (2.20)$$

where the averaged net dissipation of energy is supplied by divergences of the pressure work term through the upper and lower boundaries, $[\overline{\rho w}]_{z_1}^{z_2}$, by vertical advection of kinetic energy, $[\rho E w]$, and from conversion of tidal potential energy.

Wunsch & Ferrari suggested that vertical advection of horizontal kinetic energy is negligible, but were unable to provide a proof. This leaves us with the following balance in the abyssal interior:

$$\iint_A \mathrm{d}A \left[\overline{\rho w}\right]_{z_1}^{z_2} + \iiint_V \mathrm{d}V \overline{\mathbf{u} \cdot \nabla \Phi_{\mathrm{tide}}} \approx \iiint_V \mathrm{d}V \overline{\rho \epsilon}. \tag{2.21}$$

Wunsch & Ferrari claimed that the primary source of the vertical component of pressure work comes from waves, either internal gravity or quasi-geostrophic (Rossby waves or eddies). It was noted that these quasi-geostrophic motions mainly consist of vertical standing modes which have zero vertical flux divergence; this term is probably provided predominantly by internal gravity waves, a topic which we will discuss shortly.

2.4 Energy Sources for the Global Ocean

Given the work that we have reviewed so far, it is possible, e.g. Huang (1999), Wunsch & Ferrari (2004), to identify only a very limited number of processes which can supply the energy required to maintain the oceanic stratification. These are wind forcing, tidal forcing, geothermal heating, buoyancy forcing and atmospheric pressure loading. We will now examine each of these processes to establish how they contribute to available energy and how much of the approximate 2 TW of required mixing energy each provides.

2.4.1 Wind Forcing

The global wind does a vast amount of work on the oceans, Lueck & Reid (1984) placing this somewhere in the range of 7–36 TW. Much of this goes into small scale motions such as surface gravity waves and turbulence in the mixed layer, e.g. Lueck & Reid (1984). These motions do not penetrate into the ocean interior and are of little consequence to the general circulation or available mixing energy. The attempts to measure how much energy the wind provides for the general circulation, e.g. Fofonoff (1981), Oort et al. (1994) rely on the assumption that this work can be calculated by

$$W = \langle \tau \cdot \mathbf{v}_g \rangle \,, \tag{2.22}$$

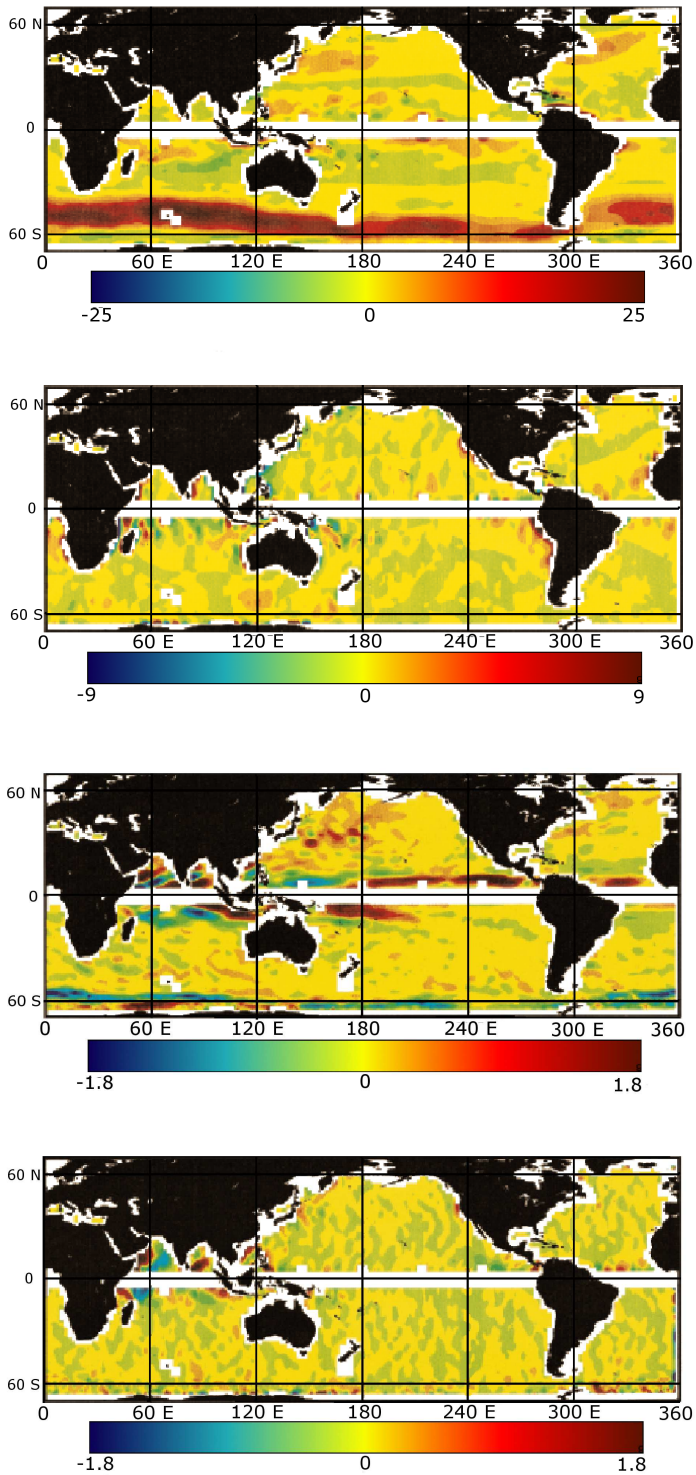

Figure 2.3: Four year average wind input and deviations from it. (a) $\langle \tau_x \rangle \cdot \langle u_g \rangle$, (b) $\langle \tau_y \rangle \cdot \langle v_g \rangle$, (c) $\langle \tau_x' u_g' \rangle$, (d) $\langle \tau_y' v_g' \rangle$. All units are Wm^{-2}. Adapted from Wunsch (1998).

the time averaged scalar product of surface horizontal wind stress, τ, and surface horizontal geostrophic velocity, $\mathbf{v}_g$. Due largely to a lack of data, many of these studies have been very crude, and hence are likely to be inaccurate. For example, the study in 1994 by Oort et al relied on ship drift data to compile a geostrophic velocity and wind climatology to obtain wind stresses. This study, as that of Fofonoff before, arrived at a value 2 TW of work on the general circulation (a huge amount when one considers that only just over 2 TW of mechanical mixing energy is required to sustain the circulation).

Wunsch (1998) used the same approach, but split the work into mean and fluctuating parts,

$$W = \langle \tau \rangle \cdot \langle \mathbf{v}_g \rangle + \left\langle \tau' \cdot \mathbf{v}'_g \right\rangle , \tag{2.23}$$

and analyzed the wind input using the TOPEX/POSEIDON ten day averaged altimetry data and wind stresses from NCEP averaged over the same ten day period. This averaging obviously would have removed all of the short timescale fluctuations from the wind data; however, due to the vast difference in timescales between atmospheric and oceanic motions, these are unlikely to contribute a significant amount of energy to the general circulation. This is well demonstrated in Figure 3.6. The deviations τ' and $\mathbf{v}'_g$ are those from the four year mean. Figure 2.3 shows the four year mean $\langle \tau_x \rangle \langle u_g \rangle$ and $\langle \tau_y \rangle \langle v_g \rangle$ and the deviations $\langle \tau'_x u'_g \rangle$ and $\langle \tau'_y v'_g \rangle$ from it. Notice the massive input from the zonal wind in the Southern Ocean (Wunsch calculated over 70% of wind input occurs south if 40° S). The effects of this can be seen in Figure 2.1. The Ekman processes driven by this intense wind cause an outcropping of isopycnals in the Southern Ocean, allowing an upwelling of dense water without the need for deep mixing. This was clearly ignored in Munk's 1966 study, and has continued to be in many since.

Wunsch arrived at a figure of just under 1 TW of wind input available to the general circulation. While this was only one-half of the figure from previous studies, it was not inconsistent with them due to the large uncertainties involved, particularly in the earlier studies. Munk & Wunsch (1998) estimated wind input as 1.2 TW to close their tidal energy budget. The 0.2 TW added to Wunsch's estimate was supposed to penetrate the surface mixed layer and directly generate internal gravity waves in the abyss. It is unknown how much of the energy imparted into the general circulation by the wind becomes available for mixing in the abyss.

How does the wind impart energy to the general circulation? Wunsch & Ferrari (2004) noted that one cannot define a unique pathway by which atmospheric kinetic energy is transferred into the oceans. Any wind stress on the surface will cause in an Ekman process, generating a finite vertical velocity, w_E. This results in an upward or downward deflected isopycnal which will raise or lower the potential energy of the ocean respectively. However, by geostrophic balance

$$\mathbf{u}_g = \frac{1}{\rho f}\hat{\mathbf{k}} \times \nabla p, \tag{2.24}$$

such a pressure anomaly will result in a circulation; the wind imparts both kinetic and potential energy into the ocean. By scaling (2.24), one can see that the ratio of the kinetic and potential energy supplied depends on the horizontal scale of the motion.

2.4.2 Tidal input

It is well known from astronomical observations and measurements that 2.5 TW of power is available from the semi-diurnal tide, M_2, with a total input from the Moon and Sun of some 3.7 TW. Of this 3.5 TW is thought to be available to the oceans, the rest being dissipated in the atmosphere or ground. Much of this remaining energy is thought to dissipate in the bottom boundary layer (bbl) of shallow marginal seas, where tidal velocities are generally of the order of 0.5 ms^{-1}, compared with 10^{-2} ms^{-1} in the open ocean. Dissipation, d, in the bottom boundary layer is given by

$$d = c_d \rho \left\langle u_{\mathrm{tidal}}^3 \right\rangle \ \mathrm{Wm}^{-2} \tag{2.25}$$

where c_d is a drag coefficient approximately equal to 0.0025. This cubic dependence led Munk & Wunsch to conclude that 1% of the ocean is responsible for over 99% of the tidal dissipation. Once they had discounted what is dissipated in the shallow bottom boundary layer, approximately 0.9 TW remained and is available to maintain the stratification in the open ocean. Of this 0.2–0.6 TW is assumed to go to the generation of internal tides and waves through interactions with bottom topography. These can be radiated away from their source, perhaps explaining the remarkably uniform mixing in the open ocean, or generating local

areas of intense mixing through further interactions with topography.

2.4.3 Geothermal Heating

Geothermal heating is a very efficiently placed source to provide mixing energy to the oceans as it heats from below, allowing Rayleigh-Bérnard convection to take place. This process may allow a large upwelling of fluid given a relatively small heat flux through entrainment of cooler statically stable fluid with the warmer unstable fluid. The potential energy imparted to the ocean by geothermal heating is given (Huang, 1999) by

$$\Phi_{\text{geo}} = g \iint_V \frac{\overline{\rho}\alpha\dot{Q}}{c_p} z \, \mathrm{d}A, \tag{2.26}$$

where $\overline{\rho}\alpha\dot{Q}/c_p$ is the buoyancy flux through the bottom boundary, $\overline{\rho}$ the average density, $\alpha = 1.67 \times 10^{-4}$ K^{-1} is the thermal expansion coefficient, c_p is heat capacity at constant pressure and $\dot{Q}$ is the heating rate.

New rock is produced at the mid-ocean ridges and over time moves away and cools. The heat flux through the rock is related to its age. Stein & Stein (1992) derived an empirical formula for calculating the age of rock on the sea bed:

$$\begin{aligned} t &= \sqrt{\frac{d - 2600}{3.65}} && \text{if } d \leq 4291.7 \text{ m} \\ t &= \frac{-\ln\left[(5651 - d)/2473\right]}{0.0278} && \text{if } d \geq 4291.7 \text{ m.} \end{aligned} \tag{2.27}$$

Here d is the depth of the sea floor and t is the age of the rock in Myrs (1 Myr $\equiv 10^6$ years). It is then possible to calculate the heat flux through the sea floor (again empirically) by the formula

$$\dot{Q} = \begin{cases} 510 t^{-1/2} & t \leq 55 \\ 48 + 96 e^{-0.0278t} & t \geq 55. \end{cases} \tag{2.28}$$

If the depth is greater than 5651 m then the heat flux is fixed at 48 mWm^{-2}.

Using the NOAA ocean topography data ($1^\circ \times 1^\circ$ resolution) Huang calculated a total global geothermal heat flux of 0.5 TW, however, this has since been corrected to 0.05 TW. It is unclear whether such a value is significant with regard

to the mixing energy required to support the general circulation. It is clearly only a small fraction of the 2 TW of energy input required, however as a source heating from below it is very well placed for mixing. The value of 2 TW of energy input required is also highly uncertain and could be as low as 1 TW, in which case such an input would be difficult to exclude from consideration. Perhaps the most interesting question regarding geothermal input is its relevance in paleo-oceanography. In the past the continents had a vastly different configuration and heat flux through the ocean floor may have been much larger. Geothermal heating, should be in the mind of anyone wanting to run an ocean model in prehistoric times.

2.4.4 Buoyancy Forcing

Buoyancy forcing occurs in two forms: thermal forcing and salinity forcing, through transport of fresh water. Given Sandström's Theorem and the no-turbulence theorem of Paparella & Young, we would expect that the net contribution of these to the potential energy of the oceans to be small, or even negative.

Surface heating increases the potential energy of the ocean by causing the fluid above the thermocline to expand, raising the centre of mass of the fluid. Conversely, cooling at the surface causes the fluid in the surface layer to contract, lowering the centre of mass and thus the potential energy of the system. One would expect that taking a sufficiently long time average in a stable climate this energy input and removal would exactly cancel out so thermal forcing would have no net effect on the energy of the oceans. However, there is a correlation between heating rate and depth of the mixed layer. Generally speaking, cooling occurs in the winter when, due to an increased wind stress and boundary layer turbulence, the mixed layer is at its deepest. Cooling is therefore more efficient at removing potential energy than heating is at injecting it, so the net contribution from thermal forcing is slightly negative. Exactly how much energy is removed through this process is unknown, as the diurnal cycle and individual strong storm events introduce great complications into the calculation. When compared to the wind and tidal inputs, however, the numbers involved here are very small and involve relatively large uncertainties; these contributions are generally assumed to be zero when making large scale budgets (Wunsch & Ferrari, 2004).

In the time average, water evaporates in the tropics, lowering the centre of mass of the ocean here, with a corresponding amount of precipitation increasing the potential energy in the high latitudes through an elevation in the free surface. During its transport, however, the fresh water loses heat to the atmosphere, the overall effect of this process is to lower the energy of the oceans. Huang (1998) estimated the net work through fresh water transport at -10^{-2} TW as a global average. Again, due to the large relative uncertainties involved, this is generally approximated as zero when making energy budgets.

2.4.5 Atmospheric Pressure Loading

The free surface of the ocean responds to changes in atmospheric pressure loading. Jeffreys (1916) concluded that the free surface elevation change, η, could be approximated by

$$\eta(t) = \frac{-P_a'(t)}{\rho_0 g}, \tag{2.29}$$

where g is local gravity, ρ_0 the reference density and p_a' a change in the atmospheric pressure. This implies that a change of 1 hPa in atmospheric pressure give a change of approximately 1 cm in sea surface elevation. Fluctuations in atmospheric pressure can thus do work om the oceans, however due to the large cancellation between pressure fluctuations over the ocean the net work done by these variations is small. In a personal communication to Wunsch, Ponte estimated the work done by atmospheric pressure loading to be around 10^{-2} TW. Due to the large uncertainties in producing energy budgets for the oceans, such a small value is usually estimated as zero.

2.5 Mixing by the General Circulation

We have seen that the two main sources of energy to the oceans are the tides and the wind field, the former providing 3.5 TW of energy input to the oceans, of which 1–2 TW is available for mixing, and the latter providing approximately 1.4 TW of energy, with over half going directly into the general circulation. A question which therefore need to be addressed is how much of the energy from wind input becomes available for mixing through dissipation of the general circulation and what are the processes responsible for this dissipation. Two processes

are apparent which can convert the kinetic energy in the general circulation into the potential energy required to maintain the stratification. The first is a loss of balance resulting in stirring through the generation of mesoscale and smaller eddies by baroclinic instability. Little is known about this, and no estimates of the rate of dissipation are available. It is thought, however, that little mixing is contributed by eddy stirring and we will use 0.1 TW as an upper bound.

Mixing can also be introduced through the turbulent field generated by the viscous dissipation of the general circulation at the ocean floor, particularly in areas of complex bottom topography, where intense mixing can take place (for example the value of $K = 100$ m^{2}s^{-1} in Table 2.1 over the Romanche Fracture Zone). However the vertical extent of such intense mixing regions is fairly limited, for example an extent of approximately 500 m in the Romanche Fracture Zone was recorded, and areas of such complex topography make up only a small fraction of the total area of the sea bed, which are dominated by smooth abyssal plains. Wunsch & Ferrari used the value of $\epsilon_p \approx 1.8 \times 10^{-9}$ W/kg from obtained from the study of Ferron et al. (1998) of the Romanche Fracture Zone, and estimated the fraction of the ocean where such intense mixing could take place to gain an estimate of the total mixing energy supplied by the general circulation. They estimated a value of 0.1 TW, but again the error bar could be huge.

2.6 Summary of the Energy Cycle in the Ocean

The vast majority of energy input into to oceans is provided by the lunisolar tides and the wind field, the former providing 3.5 TW of energy input and the latter some 20 TW, of which approximately 19 TW remains in the surface layer, producing surface gravity waves and mixing the upper ocean. Of the 3.5 TW of tidal input, 2.6 TW is dissipated in shallow marginal seas with the remaining 0.9 TW producing internal tides which in turn spend 0.1 TW of work generating internal waves. A further 0.6 TW of input is imparted to the internal wave field directly by the wind field, leaving 0.8 TW of wind input into the general circulation. The internal wave field produces the mixing in the open ocean, accounting for approximately 0.2 TW of mixing energy, and another 0.5 TW through turbulent mixing at the boundaries. The internal tides also cause turbulent mixing at the boundaries, accounting for a further 0.8 TW of mixing. The remaining 0.2 TW

required for the maintenance of the stratification is provided from drag of the the general circulation, 0.1 TW directly and 0.1 TW from mesoscale eddies. It should be noted that the figures we are using here are just the generally accepted values, and the uncertainties are hopelessly large – "at least factors of 2 and possibly as large as 10." (Wunsch & Ferrari, 2004).

Chapter 3

A Two Layer Model of the Thermohaline Circulation

In the previous sections we have seen that two of the most important factors in controlling the thermohaline circulation are wind input, most of which goes into the Southern Ocean, and vertical mixing which is essential to maintain the oceanic stratification. We now present some original calculations and analysis of a variation of a model first proposed by Gnanadesikan (1999), which includes both of these factors in a simple and highly idealized model of the thermohaline circulation, in an attempt to gain a better understanding of how there factors affect the circulation. The model involves three key processes, namely northern hemispheric sinking, low latitude upwelling and an Ekman driven upwelling in the Southern Ocean, partially balanced by an eddy return flow. These processes are parameterized in terms of the depth of the pycnocline, an area of the ocean where density rapidly increases with depth, and which generally delineates the surface mixed layer from the abyssal ocean.

3.1 Formulation

The ocean is assumed to consist of two layers, a surface layer and the abyssal ocean which are separated by the pycnocline. The setup Gnanadesikan used, shown in Figure 3.1, was justified by an observational section of the potential density in the Atlantic Ocean. Throughout most of the ocean, the pycnocline is approximately horizontal (constant depth), extending to the surface in an ap-

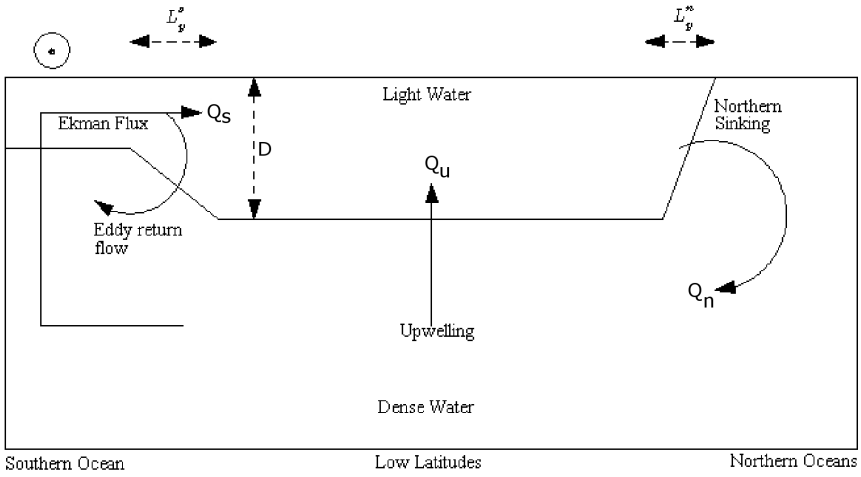

Figure 3.1: Schematic of Gnanadesikan's model of the thermohaline showing the key processes involved. The dotted circle above the Southern Ocean represents a zonal wind stress.

proximately linear fashion in the high latitudes in the northern and southern hemispheres. Any formation of deep or bottom water requires a transport across the pycnocline and Gnanadesikan was able to parameterize the key processes in the thermohaline circulation in terms of the constant depth pycnocline.

Water in the surface layer flows north, cools due to heat exchange with the atmosphere, and is rendered convectively unstable. This newly dense water then sinks across the pycnocline as North Atlantic Deep Water (NADW). A mixing rate which is constant throughout the abyss is assumed, allowing some of this NADW to rise in the low latitudes. The steady state balance is completed by the Ekman driven upwelling minus the eddy induced return flow.

3.1.1 Northern Hemisphere Sinking

We assume that the norther sinking, Q_n, is approximately equal to the northerly geostrophic transport,

$$Q_n \approx \int_{x_w}^{x_e} h v_g \, \mathrm{d}x, \tag{3.1}$$

where h is the depth, v_g the meridional geostrophic velocity and x_e and x_w are the eastern and western boundaries respectively. Then by the shallow water

approximation, assuming weak flow at depth,

$$Q_n \approx \int_{x_w}^{x_e} h \frac{g'}{f} \frac{\partial h}{\partial x} \, \mathrm{d}x, \tag{3.2}$$

where $g' = g\Delta\rho/\rho$ is the reduced gravity and f is the Coriolis frequency at the sinking latitude (at 60° N, $f \approx 1.8 \times 10^{-4}$ s^{-1}). By the chain rule we then have

$$Q_n \approx \frac{g'}{f} \int_{x_w}^{x_e} \frac{\partial}{\partial x} \left(\frac{h^2}{2} \right) \, \mathrm{d}x, \tag{3.3}$$

hence

$$Q_n \approx \frac{g'}{f} \frac{D^2}{2} \tag{3.4}$$

where D is the depth of the pycnocline. This assumes that the isopycnals outcrop on the western boundary but not on the eastern boundary, as observed (Marshall, 2005). Gnanadesikan used a slightly different parameterization of northern hemispheric sinking which arose through considering the balance between the pressure gradient in the North Atlantic and friction within the boundary currents, giving

$$Q_n = \frac{Cg'}{\beta L_y^n},$$

where β is the meridional derivative of the Coriolis parameter, f, and C is a constant which "incorporates effects of geometry and boundary layer structure." The two parameterizations produce only a minor discrepancy between results.

3.1.2 Southern Ocean Upwelling

The upwelling in the Southern Ocean, Q_s, is simply parameterized as the northerly Ekman flux driven by a zonal surface wind stress τ is the Drake Passage latitudes. This is given by

$$Q_s = \frac{\tau L_x}{\rho f}, \tag{3.5}$$

where L_x is the circumference of the Earth in the Drake Passage latitudes. Note that this has no dependence on the depth of the pycnocline.

Gnanadesikan parameterized the eddy return flow, which exports fluid from the low latitudes to the Southern Ocean, so eddy velocity $v_{\text{eddy}} = A_i \partial S/\partial z$, where S is the meridional slope of the upper layer, D/L_y^s, following Gent & McWilliams

(1990). Combining this with (3.5) gives the total return flow from the Southern Ocean:

$$Q_s = \left(\frac{\tau}{\rho f} - \frac{A_i D}{L_y^s} \right) L_x. \tag{3.6}$$

3.1.3 Interior Upwelling

The parameterization for low and mid latitude upwelling come from the Munk (1966) balance between advection and diffusion, (2.6). This yields

$$Q_u = \frac{K_v A}{D},$$

where K_v is the diapycnal diffusivity in the abyss and A the area over which the upwelling occurs.

3.1.4 Volume Balance

By conservation of volume we must have

$$Q_s + Q_u - Q_n = A \frac{\partial D}{\partial t},$$

and thus

$$\frac{\partial D}{\partial t} = \frac{\tau L_x}{A \rho f} - \frac{A_i L_x}{A L_y^s} D + \frac{K_v}{D} - \frac{g'}{2Af} D^2. \tag{3.7}$$

In a steady state, this reduces to

$$Q_u D = (Q_n - Q_s) D, \tag{3.8}$$

or equivalently

$$\frac{g'}{2f} D^3 + \frac{A_i L_x}{L_y^s} D^2 - \frac{\tau L_x}{\rho f} D - K_v A = 0, \tag{3.9}$$

a cubic equation in D, the depth of the pycnocline.

3.1.5 Model Parameters

Before we can find solutions to the model, there are a number of parameters which need to be fixed, or at least bounded. Most of these are taken from Gnanadesikan (1999), where $g' = 0.01$ ms^{-2}, $L_y^n = L_y^s = 1500$ km, $L_x = 25000$

km, and $A = 2.44 \times 10^{14}$ m^2. The Southern Ocean wind stress, τ, is of course variable, however it is believed to lie between 0.1 and 0.2 Nm^{-2}. In this study values of τ ranging from 0 to 0.3 Nm^{-2} will be used, with a standard value of 0.1 Nm^{-2}. The Southern Ocean eddy diffusivity parameter, A_i, is poorly determined. Estimates have ranged from 100 to 3000 m^{2}s^{-1} (see Gnanadesikan (1999), Note 10), although it is believed to lie at around 1000 m^{2}s^{-1}. Values ranging from 0 to 2500 m^{2}s^{-1} will be used in this study, with a standard value of 1000 m^{2}s^{-1}. The high value of eddy diffusivity in the Southern Ocean arises due to the large shear produced by the Antarctic Circumpolar Current (ACC), which can lead to velocities of over 2 ms^{-1}. The ACC is almost completely wind driven, thus over sufficiently long periods of time one would expect there to be a correlation between the Southern Ocean wind stress and the eddy diffusivity.

Determining what value to use for the diapycnal diffusivity, K_v, is less straightforward. As we have seen previously, there exists a dichotomy between the mixing rate measured in the open ocean and the rate which is supposed to be required to support the observed circulation. The discrepancy between these rates is believed to be made up by greatly enhanced mixing at the boundaries. An important question which must be addressed here is which value of diapycnal diffusivity should be used in this model? Such a simple model cannot represent the different diffusivities, so we must choose which to use. Instinctively, one would tend to use the diffusivity which must exist to support the circulation. In this two layer ocean, however, the diffusivity which is important is that which is responsible for raising fluid across the pycnocline. We would therefore be led to believe that it is the open ocean value of diapycnal diffusivity which is relevant. Whichever is the case, it is clear that the processes by which lateral homogenisation occurs are important here, even though they are not present in the model. In this study we will consider a wide range of values for K_v, which will account for open ocean mixing (where $K_v = 10^{-5}$ m^{2}s^{-1}) and implied mixing where the diapycnal diffusivity is an order of magnitude larger. We will also consider the response of the ocean in the case where diapycnal mixing is negligible.

3.2 Solutions in Limiting Scenarios

In a steady state, the model, as shown in (3.9), is a cubic polynomial, thus analytic solutions can be found. These solutions, however, are very complicated and shed very little light on the dynamics or sensitivities of the model. However, by considering the responses of the model in the limits where certain processes become unimportant it is possible to gain some insight into the interactions between the remaining processes. Gnanadesikan (1999) briefly discussed some of these ideas, particularly the scaling when Q_s is identically zero. Here that work is expanded and built upon.

3.2.1 In the Limit of no Southern Ocean Processes

If we remove the Southern Ocean from the model, the quadratic and linear terms in (3.9) disappear, so the balance is reduced to a balance between sinking in the northern hemisphere and upwelling in the low latitudes, given by

$$\frac{g'}{2f}D^3 - K_v A = 0. \tag{3.10}$$

In this regime we can see that

$$D = \gamma_D K_v^{1/3} g'^{-1/3},$$

where the pycnocline depth increases as the cube root of vertical diffusivity and decreases as the cube root of the density difference across the pycnocline in the northern hemisphere. Here $\gamma_D = (2AfK_v)^{1/3}$. We can also see that

$$Q_n = \gamma_{Q_n} K_v^{2/3} g'^{1/3},$$

where $\gamma_{Q_n} = \frac{1}{2}(2A)^{1/3} f^{-2/3}$. As this model is steady state we must have $Q_u = Q_n$. In this regime, the overturning is most sensitive to the diapycnal diffusivity. The power law is gratifyingly, though perhaps coincidentally, exactly that which has been found in experiments using full global circulation models, for example Marotzke (1997), Bryan (1987). While the model is most sensitive to K_v here, in reality this is unlikely to cause much variability in the circulation as the global average isopycnal diffusivity is only likely to change on a geological timescale,

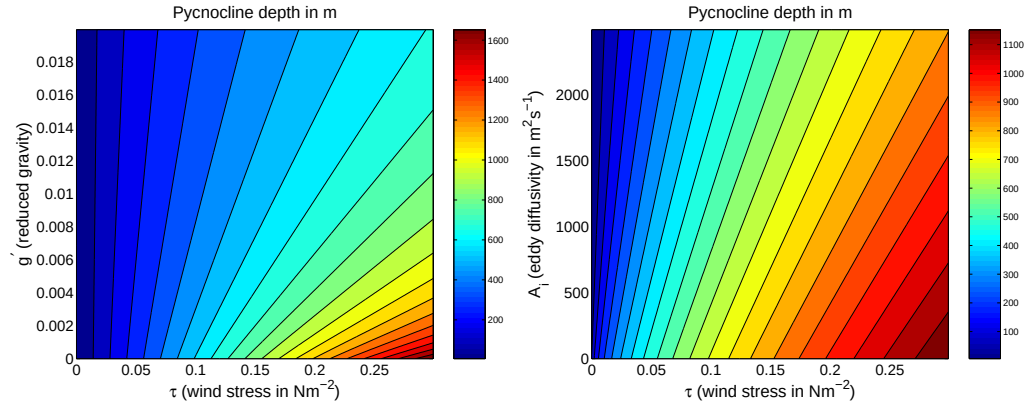

Figure 3.2: Pycnocline depth in the τ, g' parameter space [left] and in the τ, A_i parameter space [right].

if it changes at all. Therefore the variability in the circulation and structure of the thermohaline circulation in this regime will be dominated by changes in the reduced gravity, caused by variations in the density change, $\Delta\rho$, across the pycnocline in the northern hemisphere. The process most likely to cause a significant change in $\Delta\rho$ is a change in the freshwater transport between the tropics and the pole, such as an increase in evaporation and precipitation rates or injection of freshwater at the pole due to the melting of ice. It is thought that such changes, which could be brought about as a result of climate change, could result in a 'collapse' rather than a linear decay of northern hemisphere sinking, due to a bifurcation caused by salt feedback processes not included in this model, e.g. Stömmel (1961), Marotzke & Willebrand (1991). Such a collapse would drastically reduce the meridional heat transport in the northern hemisphere and would have far reaching implications for the future climate state.

3.2.2 In the Limit of no Diapycnal Mixing

In the limit where $K_v \to 0$, (3.9) is reduced to the cubic

$$\frac{g'}{2f}D^3 + \frac{A_i L_x}{L_y^s}D^2 - \frac{\tau L_x}{\rho f}D = 0, \tag{3.11}$$

and we can divide through by D to obtain the quadratic eqaution

$$\frac{g'}{2f}D^2 + \frac{A_i L_x}{L_y^s}D - \frac{\tau L_x}{\rho f} = 0. \tag{3.12}$$

Note that by doing this we lose one of the solutions to (3.11), however this is simply the solution where $D = 0$, which in the case of $K_v = 0$ implies no overturning circulation. As (3.12) is quadradic, we can find two solutions, D_1 and D_2, where

$$D_{1,2} = \frac{\frac{-A_i L_x}{L_y^s} \pm \sqrt{\left(\frac{A_i L_x}{L_y^s}\right)^2 + \frac{2g'\tau L_x}{\rho f^2}}}{g'/f}.$$

Of these, only $D \equiv D_1$ is positive (i.e. a physical solution) with

$$D = \sqrt{\left(\frac{A_i L_x f}{L_y^s g'}\right)^2 + \frac{2\tau L_x}{\rho g'}} - \frac{A_i L_x f}{L_y^s g'}.$$

Clearly as no fluid is transported to the upper layer in the low latitudes this must represent a balance between the Ekman driven upwelling and the northern sinking and eddy return flow. In fact, this now turns out to be an almost completely wind driven system. As the Southern Ocean wind stress tends to zero, the pycnocline depth also tends to zero, which is the solution in which no fluid moves at all between layers. In the limit where the eddy diffusivity tends to zero, or alternatively in the approximation where $2\tau L_x/\rho g' \gg (A_i L_x f/L_y^s g')^2$, we have that

$$D = \sqrt{\frac{2\tau L_x}{\rho g'}},$$

and

$$Q_n = \frac{g'}{2f}D^2 = \frac{\tau L_x}{\rho f} = Q_s.$$

The circulation is driven entirely by the Ekman upwelling in the Southern Ocean and has no dependence at all on the density difference across the pycnocline in the northern hemisphere, although the vertical sturcture (depth of the pycnocline) is still dependent on this density difference.

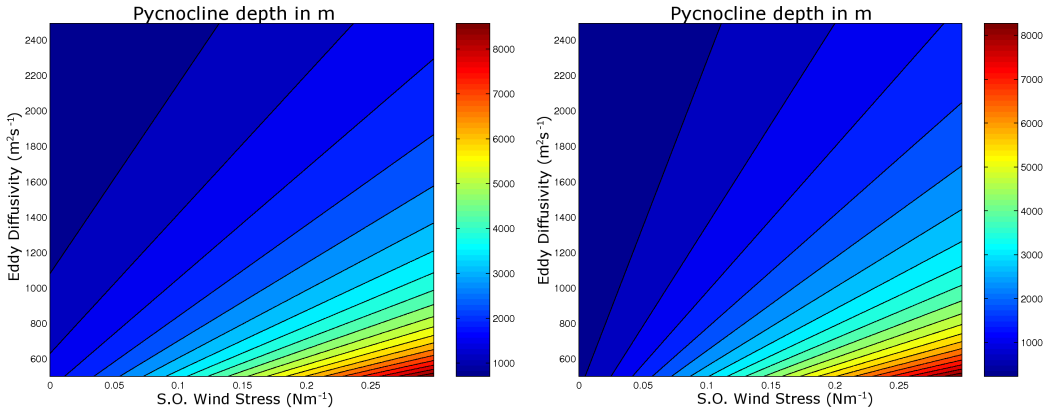

Figure 3.3: Pycnocline depth in the τ, A_i parameter space. In the left image, $K_v = 10^{-4}$ m^{2}s^{-1} and in the right image $K_v = 10^{-5}$ m^{2}s^{-1}.

3.2.3 In the Limit of no Northern Sinking

As previously noted, climate change could cause the thermohaline circulation to shut down, so it makes sense to investigate the limit where $Q_n \to 0$. In reality this would be caused by a decline or reversal of the density difference across the pycnocline in the northern hemisphere, i.e. $g' \to 0$, however for practical purposes the northern sinking (cubic) term will be removed from the model equation, leaving us with the quadratic

$$\frac{AiL_x}{L_y^s}D^2 - \frac{\tau L_x}{\rho f}D - K_v A = 0,$$

which has one physical solution, where

$$D = \frac{\tau L_y^s}{2A_i f \rho} + \sqrt{\left(\frac{\tau L_y^s}{2A_i f \rho}\right)^2 + \frac{K_v A L_y^s}{A_i L_x}}.$$

The important balance represented here is that between the Ekman driven upwelling and the eddy return flow in the Southern Ocean. As the sinking in the northern hemisphere diminishes, the only process which can remove water from the surface layer is the eddy return flow, controlled by the eddy diffusivity parameter A_i. As A_i is tightly linked to the ACC, there is no reason why it should change as northern sinking shuts down. The only way, therefore, for the eddy return flow to increase enough to enable it to balance all of the water upwelling

in the Southern Ocean and low latitudes is by a significant deepening of the pycnocline. This deepening also reduces the upwelling in the low latitudes. Figure 3.3 shows the depth of the pycnocline when $Q_n \equiv 0$ in the τ, A_i parameter space. Notice that in much of the space the pycnocline obtains an unrealistically large depth. This is necessitated in order to remove fluid from the surface layer in the limit $\tau/\rho f \rightarrow A_i/L_y^s$. Figure 3.3 also shows that when K_v is small, the pycnocline depth is more sensitive to wind stress, particularly when this is also small. This can be seen directly from the physical solution to (3.12). When τ becomes small, the $(K_v A L_y^s/A_i L_x)^{1/2}$ term comes to dominate the balance. The smaller K_v becomes, therefore, the more sensitive the model becomes to wind stress.

3.3 Full Solutions

Having considered all of the relevant limiting scenarios, we can now see where these fit into the full solutions, which are shown in the τ, K_v parameter spaces in Figures 3.4 and 3.5 respectively. As expected, when K_v is small, low latitude upwelling also becomes small, and insensitive to any other parameters. The combined Southern Ocean processes are insensitive to K_v over most of both parameter spaces, despite the face that each of the constituent Southern Ocean processes (Ekman upwelling and eddy return flow) are each dependent on K_v.

3.4 Time Dependent Solutions

When all of the parameters are held constant, the model simply tends to equilibrium on a timescale of a few hundred years. However, time dependent solutions can also be used to demonstrate that high frequency wind fluctuations have little impact on the general circulation, as assumed by Wunsch (1998) when estimating the wind input into the general circulation.

The model is solved using a third order Adams-Bashforth linear multistep method, with a third order Runge-Kutta method used to generate the starting values. A stochastic wind stress is generated using uniformly distributed pseudo-random numbers. The results for two such integrations are shown in Figure 3.6. The pycnocline depth is well correlated with the wind stress, although it lags behind it be a few hundred years. However, only low frequency fluctuations in the

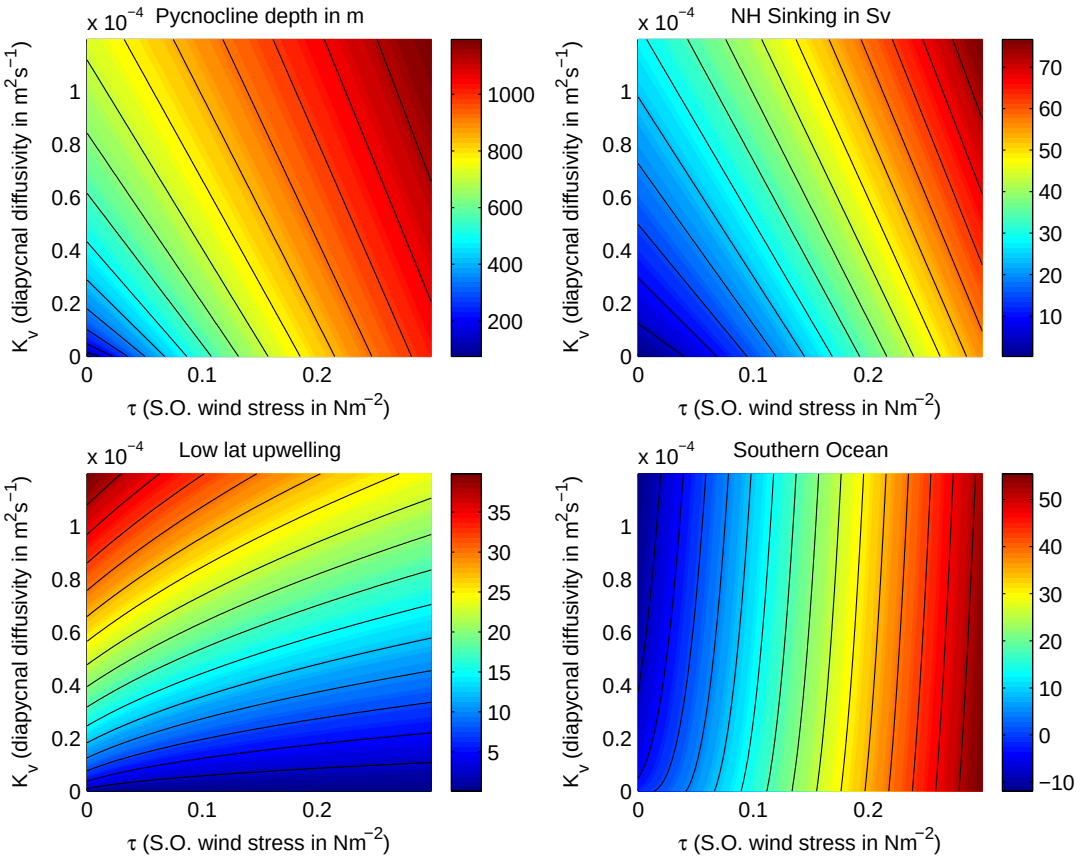

Figure 3.4: Pycnocline depth, northern hemisphere sinking, low latitude upwelling and Southern Ocean upwelling/sinking for the full model equation in the τ, K_v parameter space.

wind stress are mirrored in the pycnocline depth, with the high frequency fluctuations being filtered out by the ocean. This strongly suggests that short time scale variability in the wind field has a negligible effect on the general circulation of the oceans.

3.5 Multiple Equilibria

Does this model support multiple equilibria? Unlike some other simple models of the thermohaline circulation, such as Stömmel's two box model, this model does not include any sort of fresh water transport or haline feedback. One might therefore expect that it will not support multiple equilibria, and this is indeed

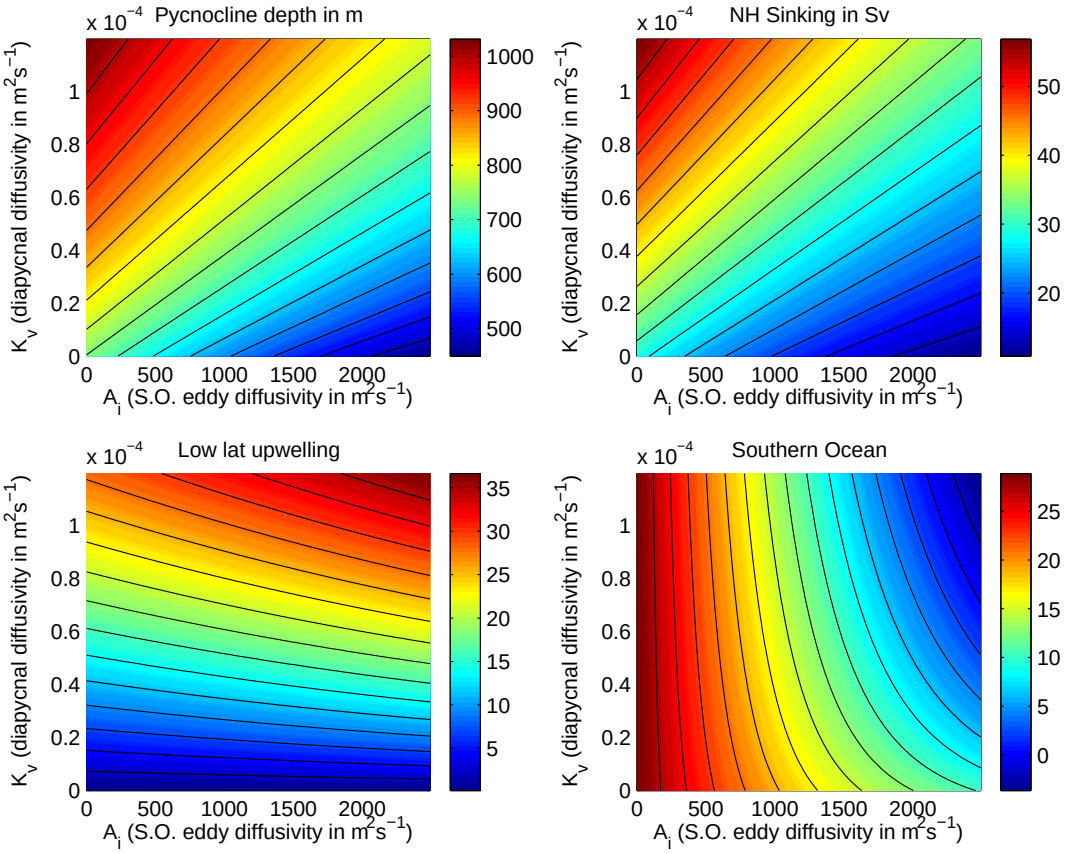

Figure 3.5: Pycnocline depth, northern hemisphere sinking, low latitude upwelling and Southern Ocean upwelling/sinking for the full model equation in the A_i, K_v parameter space.

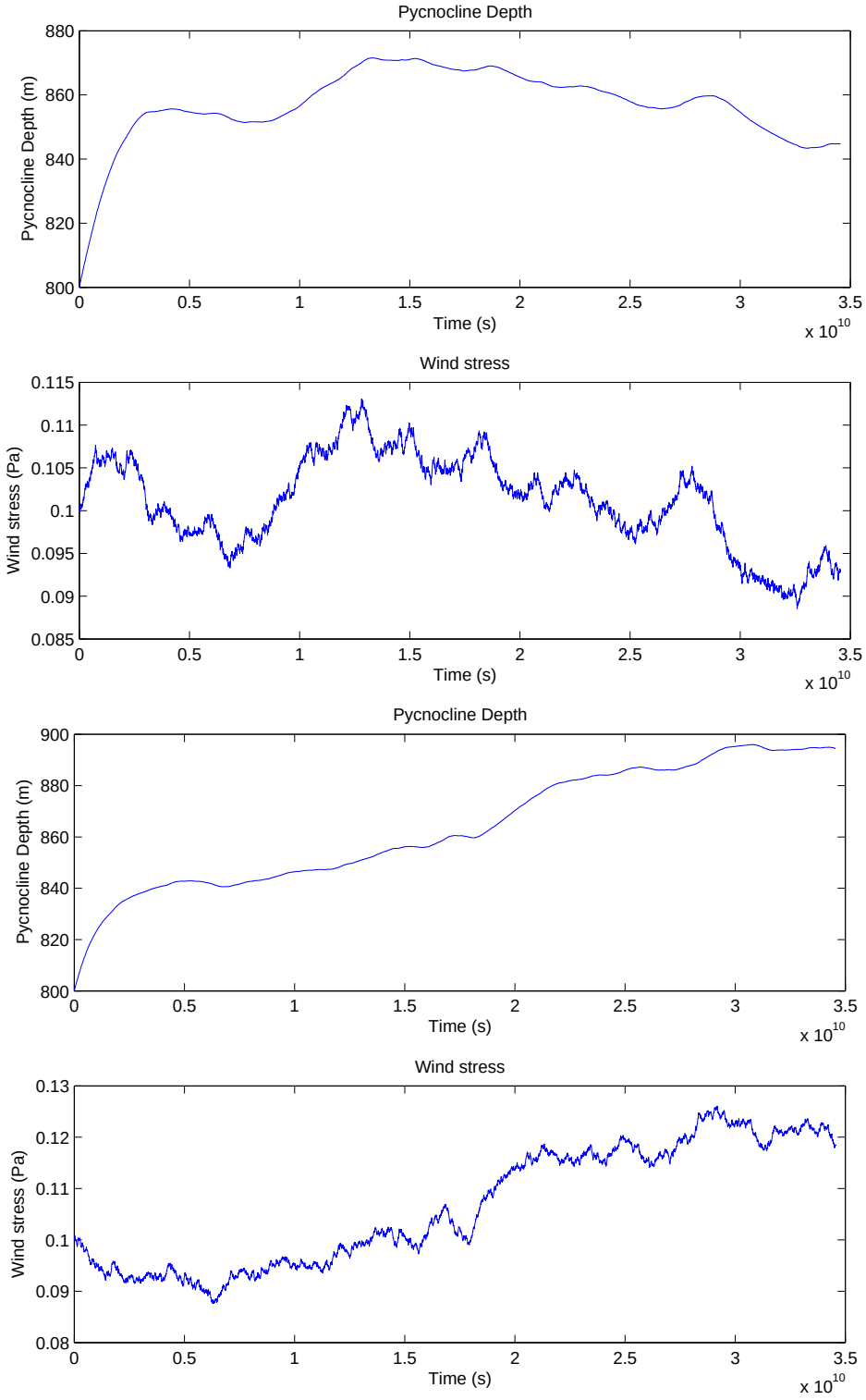

Figure 3.6: Pycnocline depth varying with two stochastic wind stresses. This demonstrates that high frequency fluctuations in the wind stress have very little effect on the general circulation.

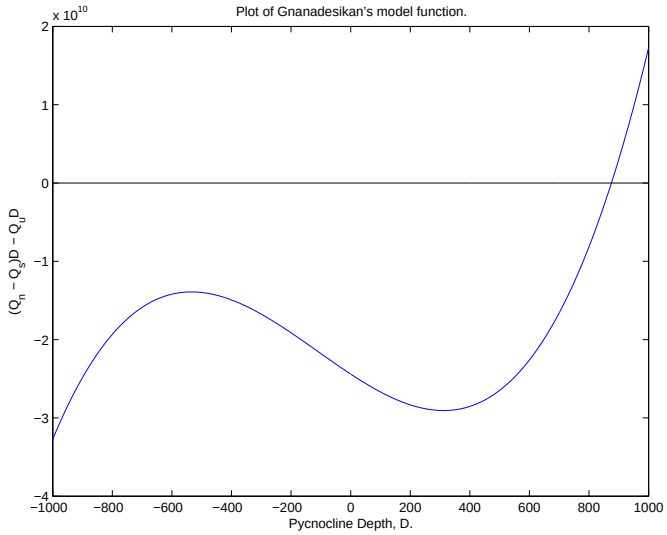

Figure 3.7: A plot of the cubic model fuction against pycnocline depth showing only one real solution. Here $\tau = 0.1$ Nm^{-2}, $K_v = 10^{-4}$ m^{2}s^{-1}, $A_i = 1000$ m^{2}s^{-1}.

found to be the case. Figure 3.7 shows the model function against pycnocline depth, and we can see that there is only one physical (i.e. non-negative, real) zero of the function, corresponding to a single stable mode of the system. There are, however, at least three terms in the equation (3.9) that are either variable or poorly quantified, namely wind stress, τ, vertical diffusivity, K_v, and Southern Ocean eddy diffusivity, A_i. Figure 3.7 shows that only one solution exists for one set of values of τ, K_v, A_i, but tells us nothing about the existence of solutions for other configurations of the model. An analytic investigation of the solutions also proves useless, as the solutions to (3.9) are horribly complicated. Instead, we carry out a numerical search for solutions between what we consider extreme values of the three variables. Typical values for τ, K_v and A_i are 0.1 Nm^{-2}, $10^{-4}/10^{-5}$ m^{2}s^{-1} and 10^3 m^{2}s^{-1} respectively. The search was carried out over the intervals 0 Nm^{-2} $\leq \tau \leq 0.5$ Nm^{-2}, 10^{-8} m^{2}s^{-1} $\leq K_v \leq 2 \times 10^{-4}$ m^{2}s^{-1}, 0 m^{2}s^{-1} $\leq A_i \leq 10^4$ m^{2}s^{-1} and no multiple, positive real roots were found. We thus conclude that this model supports at most one physical solution. Note that as (3.9) is cubic it has at least one real solution, which is positive for all realistic values of τ, K_v and A_i, thus this model has *exactly* one physical solution.

3.6 Summary

Gnanadesikan (1999) proposed a simple two layer model of the thermohaline circulation. By identifying and parameterizing a small number of processes key to the existence of the circulation in terms of the depth of the pycnocline, D, fluid transports could be found by solving a cubic equation in D.

The solutions and behaviour of this model were investigated analytically in limiting scenarios and numerically for the full equation. It was shown that when Southern Ocean processes are neglected the circulation strength follows a power law found in other work involving numerical general circulation models, for example Marotzke (1997), Bryan (1987). It is unclear whether or not this is coincidental. When interior upwelling was neglected, it was found that, in the limit of no eddy return flow, the circulation was controlled by the Ekman upwelling in the Southern Ocean and had no sensitivity to processes in the northern hemisphere, despite the fact that the pycnocline depth remained sensitive to these processes. The limit found here was that found by Toggweiler & Samuels (1998) in an investigation into the behaviour of a general circulation model in the limit of no vertical mixing.

It was shown that for all realistic parameters the model has at least one physical solution. However it was also shown that there is at most one solution and thus the model is incapable of exhibiting multiple stable equilibria which are found in a hierarchy of other numerical and analyic models of the thermohaline circulation. This is due to the lack of any haline forcing in the model which can reduce or negate the density gradient in the North Atlantic.

Chapter 4

Multiple Equilibria in the Thermohaline Circulation

We have seen in the previous chapter that the model of the thermohaline circulation proposed by Gnanadesikan (1999) has only one equilibria for a realistic parameter set. It is widely believed, however, that opposing buoyancy forces created by gradients of temperature and salinity within the Atlantic could allow the existence of two or more stable equilibria. This theory has been supported by a wide array of numerical and analytical models, from the most simple two box models (e.g. Stömmel, 1961) to modern day coupled atmosphere-ocean general circulation models.

4.1 A Two Box Model of the Thermohaline Circulation.

Stömmel (1961) proposed a two box model of the thermohaline circulation driven by thermal and haline forcing, a simplified version of which is presented here. One box is representative of the low latitudes and the other the northern hemisphere. Each of these boxes is assumed to have a prescribed temperature T_1, T_2 and salinity S_1, S_2, with ΔT and ΔS the differences in temperature and salinity, respectively. It is also assumed that transport $q \propto (\rho_1 - \rho_2)$, and that there is some freshwater transport, E, between the low latitude and polar boxes. This situation is summerised in Figure 4.1. In a steady state, the salt budget for each

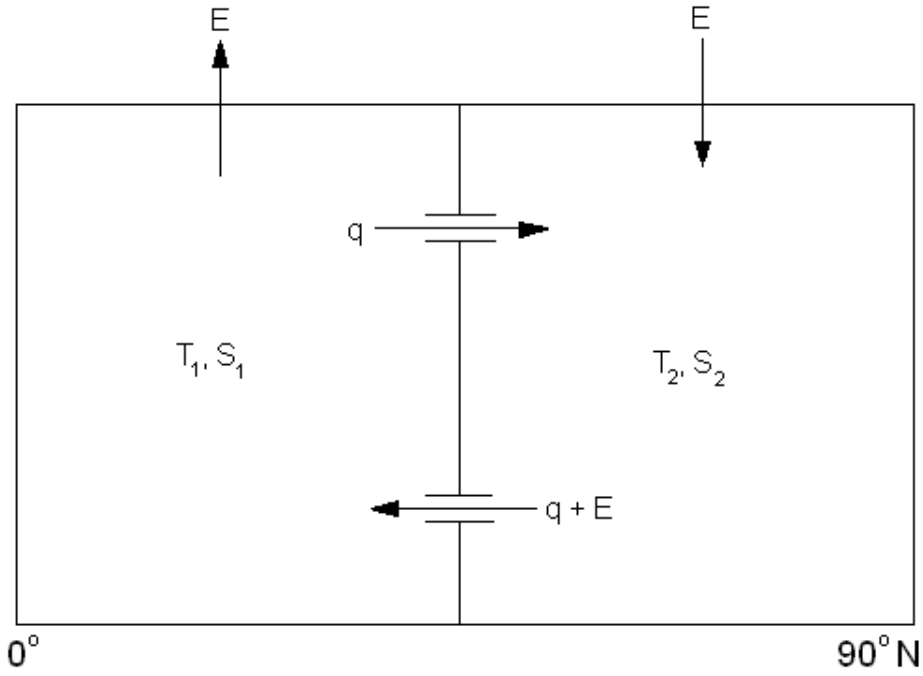

Figure 4.1: Two box, single hemisphere model of the thermohaline circulation, based on Stömmel (1961). Each box is assumed to be well mixed and have a prescribed temperature and salinity. There is also a prescribed fresh water transport, E, from the low latitude box to the polar box. The two boxes are connected with two pipes, representing deep and shallow currents.

of these boxes is given by

$$|q|S_1 = (|q| + E)\, S_2,$$

or equivalently

$$|q|\Delta S = ES_2 \approx ES_0.$$

The modulus signs are needed here as no assumptions have been made about the direction of the circulation. Assuming that the transport is a linear function of the density difference, we have

$$q = k\left(\alpha\Delta T - \beta\Delta S\right),$$

and thus

$$|q|q - k\alpha\Delta T|q| + k\beta ES_0 \approx 0. \tag{4.1}$$

The strength of the circulation is thus given by a quadratic equation in q, the transport. In the case where $q > 0$, (4.1) becomes

$$q^2 - k\alpha\Delta T q + k\beta ES_0 \approx 0,$$

which has two real root for

$$\frac{k\alpha^2\left(\Delta T\right)^2}{4\beta S_0} > E.$$

Assuming standard values of $\alpha = 2 \times 10^{-4}$ K^{-1}, $\beta = 0.8 \times 10^{-3}$ $(^0/_{00})^{-1}$, $k = 0.5 \times 10^{10}$ m^{3}s^{-1}, $\Delta T = 20$ K, $S_o = 35$ $^0/_{00}$, two real solutions exist when

$$E < 0.7 \text{ Sv (approx.)},$$

and are given by

$$\frac{k\alpha\Delta T \pm \sqrt{k^2\alpha^2\left(\Delta T\right)^2 - 4k\beta ES_0}}{2}. \tag{4.2}$$

When $E = 0$, (4.2) reduces to

$$\begin{aligned} q &= 0,\ k\alpha\Delta T \text{ Sv} \\ &= 0,\ 20 \text{ Sv}. \end{aligned}$$

In the case where $q < 0$, there exists only one real solution to (4.1). The

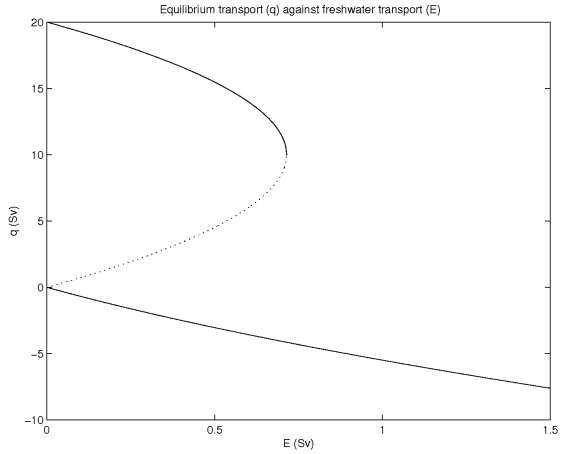

Figure 4.2: Solution of (4.1) showing multiple stable equilibria and a mechanism by which the thermohaline circulation could collapse, jumping from one stable equilibrium to the second. Solid lines show the stable equilibria and the dashed line represents an unstable equilibria.

combined solutions are shown in Figure 4.2. Here the solid lines represent stable modes of the thermohaline circulation and the dotted line represents an unstable mode. The upper solid line represents the state the thermohaline circulation is in currently, whereby a large amount fluid sinks in the northern hemisphere driven by temperature gradients between the equatorial and polar regions. However, if this circulation slows sufficiently, the fresh water transport, E, is able to change the density gradient sufficiently to cause the circulation to reverse – when the state lies on the upper branch, a sufficient increase in freshwater transport will cause the transport to follow the convex hull between the two stable modes, allowing a collapse of the circulation on a very short (decadal) timescale. A subsequent decrease in the freshwater transport would not cause the solution to jump back to the northern sinking state as the northern upwelling solution exists for all positive values of E.

An important question which needs to be answered here is how this model relates to the ideas of mixing and energy that have been discussed earlier, and whether this two box model has any relevance to the two layer model discussed earlier. At first glance it appears that this model is irreconcilable with the earlier discussion of energy in the oceans. The model, like any model, is not energy conserving, but more importantly this model seems to be driven entirely by den-

sity gradients in the fluid. Such a system, as argued by Sandström and others, can only remove energy from the fluid, and thus cannot maintain a circulation. However, when one looks back at the assumptions which have been made, the differences between the two box, the two layer and the energetic ideas are not so vast. One of the key assumptions made for the two box model is that both of the boxes are well mixed. Such an assumption means that a turbulent field within the ocean is being implied, but no energy source is related to provide this. From the earlier discussions we know that the energy required for this is provided primarily by the tides and the winds, which clearly cannot be included in such a simple model. This situation is quite similar to that in the two layer model considered earlier. Then a constant upwelling in the low latitudes, K_v, was assumed, again implying some turbulent field, and again without any associated energy source.

4.2 Multiple Equilibria in General Circulation Models

One of the first investigations into multiple equilibria in the general circulation using a coupled atmosphere-ocean general circulation model was carried out by Manabe & Stouffer (1988). They started the integration from a state where the atmosphere was dry, isothermal and at rest, and the the ocean was isothermal, at rest and had a uniform salinity. Once the model had reached a steady state, Manabe & Stouffer conducted two experiments. In the first they forced the model by restoring the surface salinities to the observed profiles on a timescale of 30 days, while in the second this forcing was not included. Two quasi-stable equilibria were found which were qualitatively similar to the two states found in the Stömmel (1961) model. The solution where the thermohaline circulation exists arose from the first experiment where surface salinities were restored, and the second equilibria, where there is no large overturning in the north Atlantic was simply achieved by integrating the model forward from the aforementioned initial conditions. That the existence of a thermohaline circulation requires the extra forcing comes as no great surprise. The sinking of the thermohaline circulation in the northern Atlantic is controlled largely by sinking of water that has become dense due to evaporation, which leaves the remaining water with a higher salinity. This evaporation is encouraged by high sea surface temperatures in the north

Atlantic which are in turn caused by the meridional heat transport caused by the thermohaline circulation itself. This 'chicken and egg' situation resulting from positive feedback mechanisms in the thermohaline circulation provides a simple physical reasoning for why the thermohaline circulation is difficult to regain once it has collapsed into another stable state.

Marotzke & Willebrand (1991) investigated equilibria in the oceans using an ocean model with idealized geometry, consisting of two equally sized, rectangular ocean basins, representing the Atlantic and the Pacific, connected by a circumpolar channel. Marotzke found the two equilibria previously known, but he also found two further equilibria, which he termed 'conveyor belts.' Marotzke's model used a very course resolution grid ($3.75^\circ \times 4^\circ$) so it is possible that there are further possible equilibria that he did not find, or that those he did find would be unable to exist in reality.

4.3 Multiple Equilibria and the Two Layer Model

Given the underlying similarities between the two box and the two layer model, and the fact that such a wide range of models predict the existence of two or more stable equilibria in the thermohaline circulation, it seems desirable to find a way to paramterize the processes in Gnanadesikan's two layer model in such a way as to allow the existence of multiple equilibria. Such an extension of Gnanadesikan (1999) is now presented.

In line with the Stömmel (1961) model, it seems that the best way to do this is to re-parameterize the northern sinking term to include the effects of a haline feedback. This can be done in a simple but non-physical way by considering the results from the two box model. It can be seen from Figure 4.2 that as freshwater transport increases, the ocean transport (equivalent to the northern sinking, Q_n) decreases steadily until a critical point is reached, where the northern sinking collapses and is replaced by a state where fluid upwells in the northern hemisphere and sinks in the low latitudes. This mode is unsupported in the two layer model, as $Q_u = K_v A/D$, which can only be negative for an unphysical (negative) pycnocline depth. However, as the two layer model contains Southern Ocean processes which are not present in the two box model, we can consider the collapsed state to be where the northern sinking tends to zero and the balance is

between the low latitudes and the southern hemisphere. In the two box model, the collapse occurs when the northern sinking falls below approximately 10 Sv. To parameterize this behaviour into the two layer model, the northern sinking term is taken to be a function not only of the depth of the pycnocline, but also of itself, so that we have $Q_n = \Psi(Q_n)\Phi(D)$. The properties required of Ψ are that $\Psi \to 1$ for $Q_n > 10$ Sv and $\Psi \to 0$ for $Q_n < 10$ Sv. It is also desirable for Ψ to be a smooth function. The form chosen for Ψ is a scaled, translated tanh function,

$$\Psi(Q_n) = \frac{1}{2}\tanh\left(\frac{Q_n - 10^7}{2\times 10^7}\right) + \frac{1}{2}.$$

The northern sinking term is then given implicitly by

$$Q_n = \left[\frac{1}{2}\tanh\left(\frac{Q_n - 10^7}{2\times 10^7}\right) + \frac{1}{2}\right]\frac{g'}{2f}D^2, \tag{4.3}$$

and the model equation becomes

$$\left[\frac{1}{2}\tanh\left(\frac{Q_n - 10^7}{2\times 10^7}\right) + \frac{1}{2}\right]\frac{g'}{2f}D^3 + \frac{A_i L_x}{L_y^s}D^2 - \frac{\tau L_x}{\rho f}D - K_v A = 0. \tag{4.4}$$

This is implicit and highly non-analytic; the steady state solutions become very hard to compute directly. It is, however, relatively straightforward to numerically solve for the time dependent evolution. The steady state solutions can then be found by integrating forwards to equilibrium. The time evolution is again solved for using a third order Adams-Bashforth linear multistep method with Runge-Kutta starting values. The initial pycnocline depth, $D(0) \equiv D_0$, was chosen to be 850 m when investigating the solution where northern sinking occurs and 1 m when investigating the collapsed circulation.

4.3.1 Steady-state Solutions

The steady state solutions are shown in Figures 4.3–4.6. Figure 4.3 shows the solution in the A_i, K_v parameter space, where the integration was started in the northern sinking state ($D_0 = 850$ m). Unsurprisingly, the solutions here are similar to those in Figure 3.4 over most of the space, however for large A_i and small K_v, the northern sinking collapses, and the solutions here differ from those in 3.4. As the circulation collapses, the net motion in the Southern Ocean

becomes a sinking of around 4 Sv, balanced by an upwelling of similar magnitude in the low latitudes, which has reduced only slightly. In the collapsed state the pycnocline depth becomes very sensitive to the Southern Ocean eddy diffusivity. This happens because in the absence of northern sinking, the only process which can remove fluid from the surface layer is the Southern Ocean eddy return flow. As the eddy diffusivity is lowered, the pycnocline depth must increase to allow a similar amount of fluid to be returned to the abyssal layer.

Figure 4.4 shows the steady-state solutions in the τ, K_v parameter space. Again the solutions are for the northern sinking solution where it exists, which is everywhere other than where τ and K_v are suitably small. Again in the collapsed state a sinking of between 5 Sv and 10 Sv in the southern hemisphere is balanced by a similar upwelling in the low latitudes. In the collapsed state the pycnocline depth is very sensitive to the wind stress and increases with it, a response necessary to allow the removal of the extra fluid upwelling into the surface layer.

Figures 4.5 and 4.6 show the steady state solutions in the A_i, K_v and τ, K_v parameter spaces when the integration was started in the collapsed state ($D_0 = 1$ m). The fact that these figures differ from Figures 4.3 and 4.4 shows that the reparameterization of Q_n has indeed introduced multiple equilibria into the model, rather than simply scaling out the northern sinking for certain sets of parameters and allowing it to recover if we then revert to the standard parameter set. This is better seen through the time dependent problem, which we will come to shortly. In the A_i, K_v parameter space, the solutions do not vary a great deal, except where both K_v and A_i are large, where the low latitude upwelling increases, balanced by a comparable increase in sinking in the Southern Ocean. When A_i becomes small the only process by which fluid can be removed from the upper layer also becomes small. In order to maintain the balance, the pycnocline must deepen significantly and rapidly becomes unphysical, obtaining a depth greater than the ocean itself. In the τ, K_v parameter space (Figure 4.6), the dominant balance is again between the Southern Ocean and the low latitudes, and these solutions are sensitive to both wind stress and diapycnal diffusivity. The pycnocline depth is deep throughout the space, and increases with increasing wind stress. The Northern hemisphere sinking is also increases with wind stress and is fairly insensitive to diapycnal diffusivity, however it remains very small throughout the parameter space.

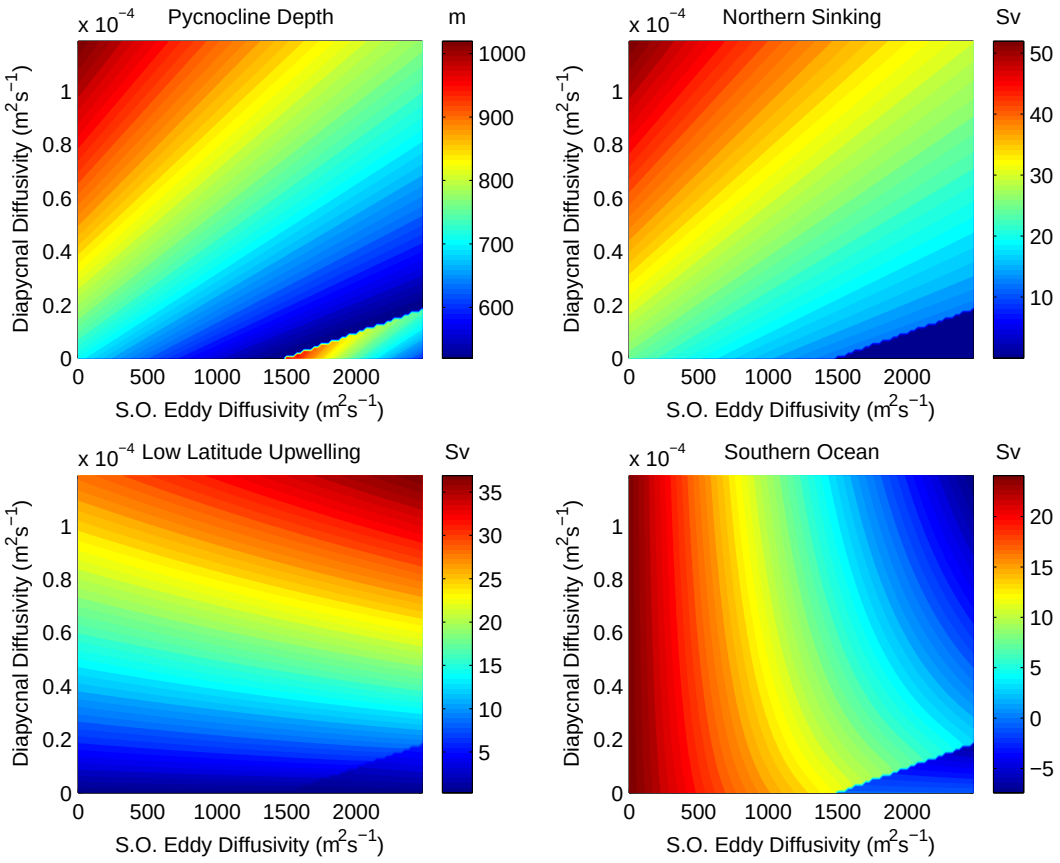

Figure 4.3: Pycnocline depth, northern sinking, low latitude upwelling and Southern Ocean upwelling/sinking in the reparameterized model which allows the circulation to collapse, in the A_i, K_v parameter space. The initial state was assumed to be the northern sinking state. This state does not exist for sufficiently large A_i and small K_v.

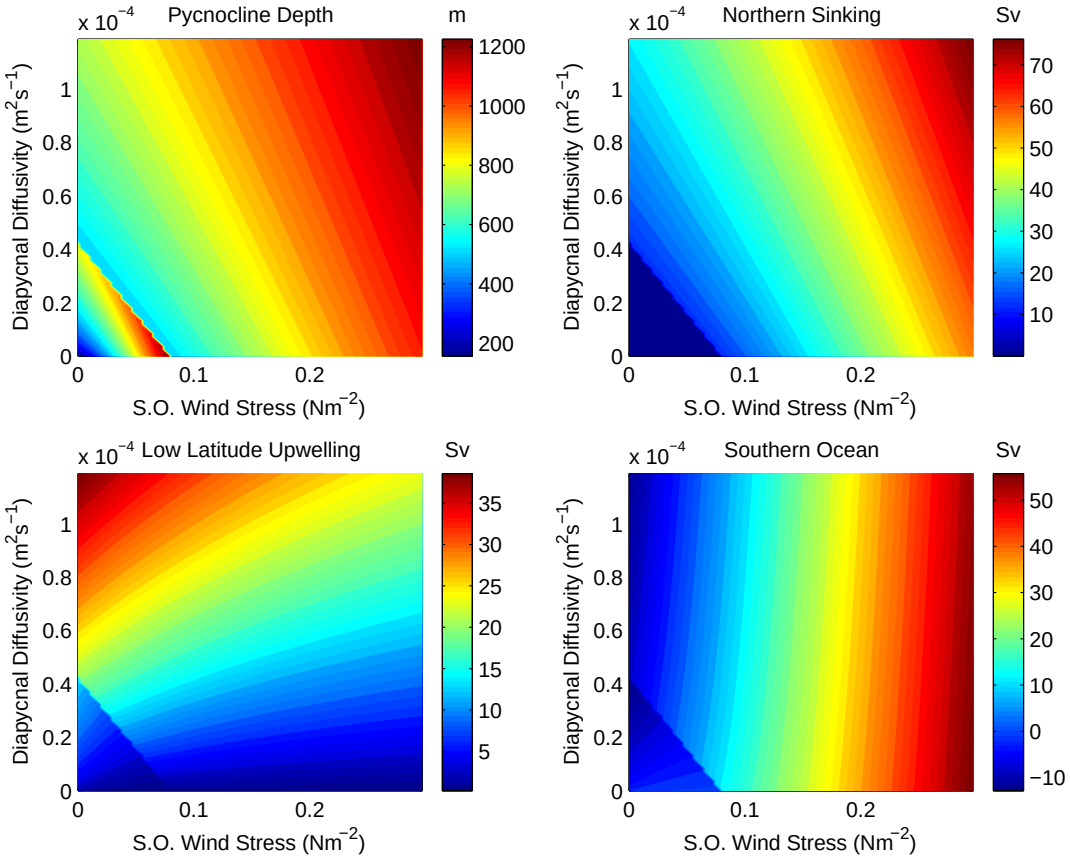

Figure 4.4: Pycnocline depth, northern sinking, low latitude upwelling and Southern Ocean upwelling/sinking in the reparameterized model which allows the circulation to collapse, in the τ, K_v parameter space. The initial state was assumed to be the northern sinking state. This state does not exist for sufficiently small τ and K_v.

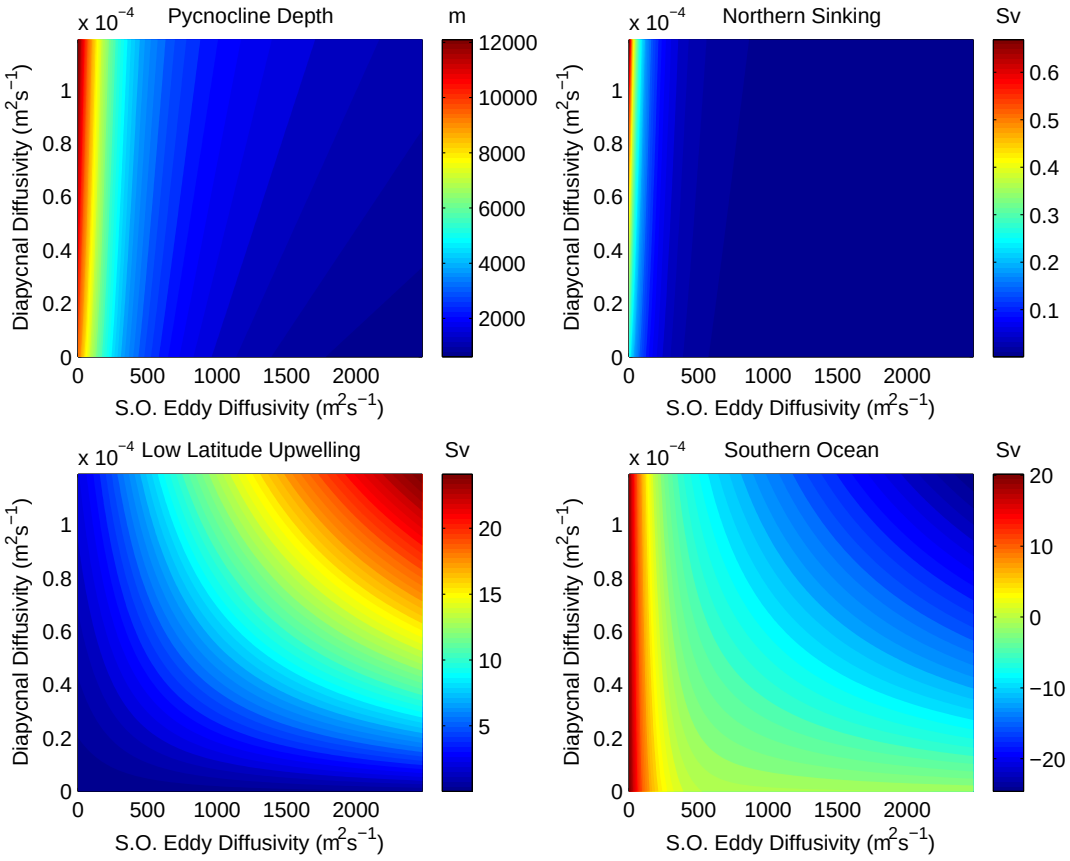

Figure 4.5: Pycnocline depth, northern sinking, low latitude upwelling and Southern Ocean upwelling/sinking in the reparameterized model which allows the circulation to collapse, in the A_i, K_v parameter space. The initial state was assumed to be the collapsed state. This state exists for all values of A_i and K_v.

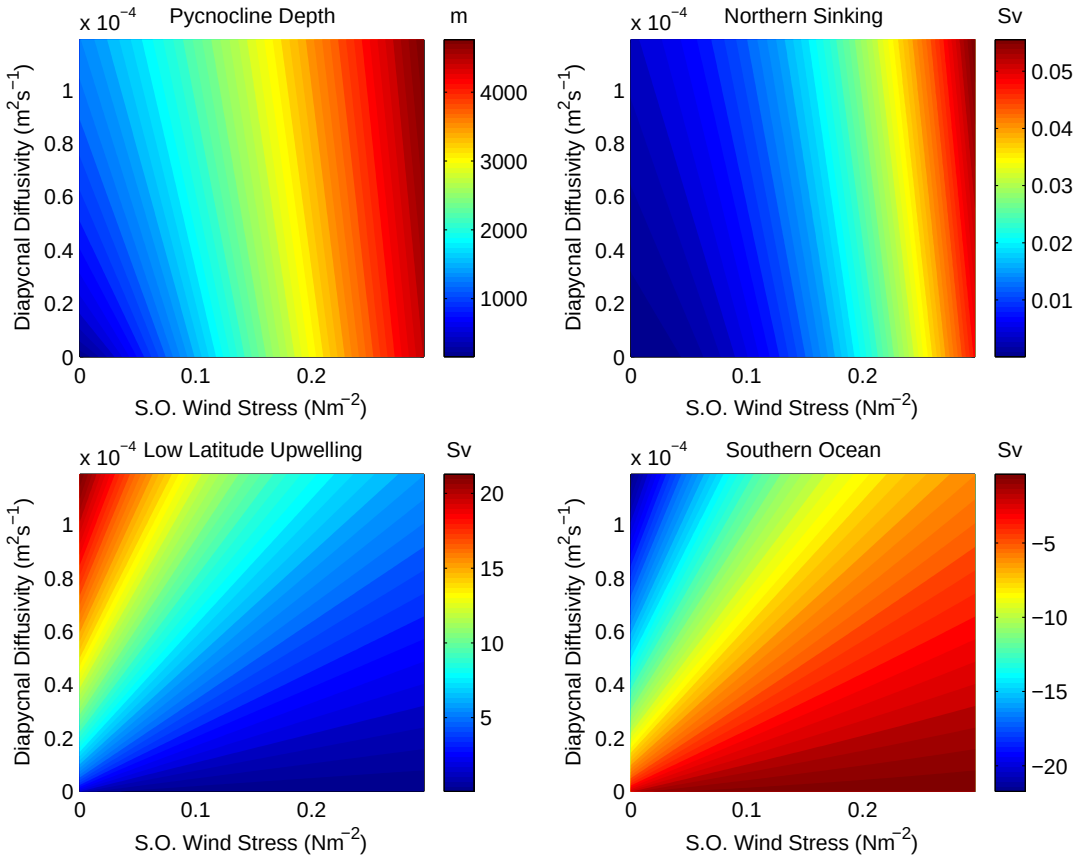

Figure 4.6: Pycnocline depth, northern sinking, low latitude upwelling and Southern Ocean upwelling/sinking in the reparameterized model which allows the circulation to collapse, in the τ, K_v parameter space. The initial state was assumed to be the collapsed state. This state exists for all values of τ and K_v.

4.3.2 A Time Dependent Experiment

To better demonstrate the multiple equilibria and the corresponding new behaviour that have been introduced into this model, the following simple experiment is considered. The model is integrated forward for 10^{11} s, or approximately 3170 years. For the first quarter of the integration, the model is allowed to reach an equilibrium, with K_v, τ and A_i held at their standard values. Then, between one quarter and three quarters of the integration, the diapycnal diffusivity and wind stress are decreased to where $K_v = 2.6 \times 10^{-5}$ m^{2}s^{-1} and $\tau = 0.026$ Nm^{-2}. After the third quarter of the integration is complete, K_v and τ are increased back to their original, standard values between three quarters and seven eighths of the integration. The results of this experiment are shown in Figure 4.7. As the diapycnal diffusivity and Southern Ocean wind stress are lowered, initially the northern sinking decreases as it would in the model described in Chapter 3. This corresponds to a decrease in the depth of the pycnocline and in the low latitude and Southern Ocean upwelling. Approximately half way through the integration, the northern sinking collapses. This collapse initially causes the pycnocline to deepen, but this is soon countered by the decreasing wind stress and diapycnal diffusivity which force it to shallow again. At $t = 7.5 \times 10^{10}$ s the Southern Ocean wind stress and diapycnal diffusivity are relaxed back to their original values over the next 1.25×10^{10} s. This causes the pycnocline the deepen significantly, reaching approximately 2000 m by the end of the integration. Initially this increase in K_v and τ causes the upwelling in the low latitudes and the Southern Ocean to increase significantly, supplying the fluid necessary for the deepening of the pycnocline. However, once K_v and τ reach their standard values and are again held steady, the low latitude upwelling is reduced and the Southern Ocean begins to enter a sinking state. By the end of the integration the model is heading towards an equilibrium where all of the fluid upwelled in the low latitudes is removed from the surface layer by the eddy return flow in the Southern Ocean, allowed by the deep pycnocline.

4.4 Summary

Gnanadesikan (1999) proposed a simple two layer model of the thermohaline circulation. While this model gave a reasonable representation of the thermohaline

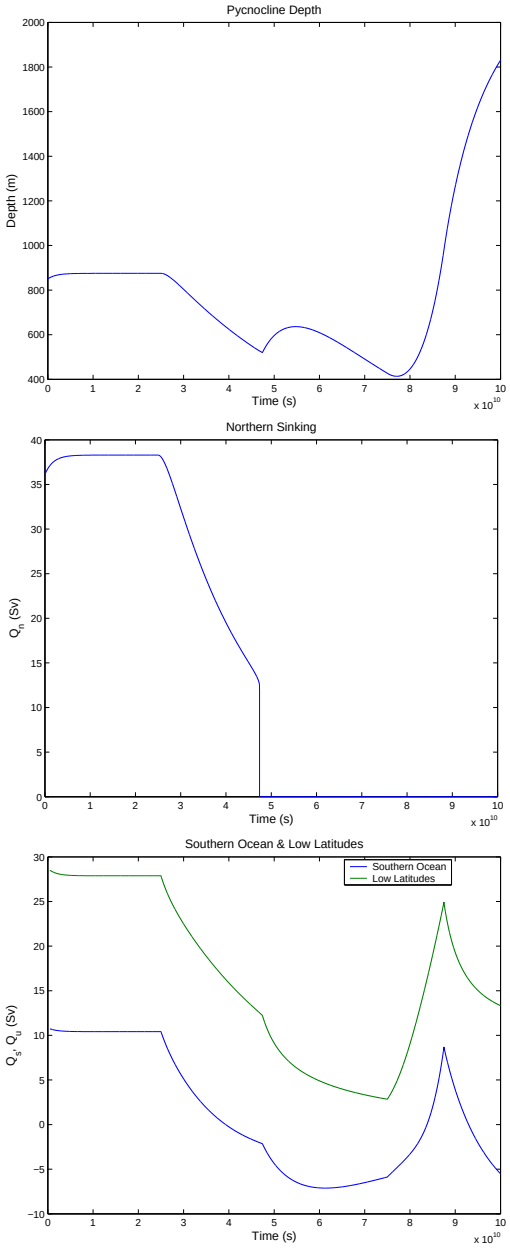

Figure 4.7: Pycnocline depth, northern sinking and low latitude upwelling and Southern Ocean upwelling/sinking over a time interval of 10^{11} s. Between $t = 0$ s and $t = 2.5 \times 10^{10}$ s, the model is allowed to tend to an equilibrium, where K_v, τ and A_i are held at their standard values. Between 2.5×10^{10} s and 7.5×10^{10}, K_v and τ are gradually lowered. The circulation collapses just before $t = 5 \times 10^{10}$ s. K_v and τ are then restored by $t = 7.5 \times 10^{10}$ s, however the circulation does not recover but the pycnocline deepens allowing a balance to form between the Southern Ocean and the low latitudes.

circulation, it did not support multiple equilibria which are observed in many other analytic and numerical ocean models.

An investigation into a version of the two box model of the thermohaline circulation proposed by Stömmel (1961) gave an approximate value that the fluid transport in the northern hemisphere must fall to for the circulation to collapse. Using this value we were able to reparameterize the northern sinking term in the two layer model to allow the two layer model to exhibit similar behaviour. This reparameterization was intended to provide a haline forcing in the model, however it was not derived on a rigorous physical basis.

While the results presented here are very preliminary, they suggest that it may be possible to reconcile the two box model of Stömmel and the two layer model of Gnanadesikan which on first inspection appear to be mutually inconsistent.

Chapter 5

Summary and Discussion

Sandström's Theorem, together with the no turbulence theorem of Paparella & Young strongly suggest that the ocean is not forced by buoyancy exchange at the surface, but rather that the energy input required to maintain the circulation comes from other sources in the from of mechanical mixing energy which maintains that stratification against the circulation. This, of course, dispels the notion of a thermohaline circulation driven by freshwater transport and heat exchange with the atmosphere.

A number of observational campaigns have been carried out to attempt to quantify how much mixing energy is required to maintain the stratification. A dichotomy arose here between those studies that implied diapycnal mixing rates by measuring flow into and out of basins and those that used microstructure measurements to measure diapycnal mixing directly. The former found the required diapycnal diffusivity to be of the order of 10^{-4} m^2s^{-1}, while the latter found rates of only 10^{-5} m^2s^{-1} over most of the ocean, a problem which became known as the missing mixing problem. The current theories suggest that the mixing in the open ocean is provided by the breaking of the internal wave field, while the rest of the mixing is provided by interactions of internal tides and waves with complex topography at the boundaries, such as the over the mid-ocean ridges.

Further observational and theoretical studies have attempted to identify the sources of mixing energy, of which analyses show around 2 TW is required. A surprising result is that much of this energy is seems to some from the lunisolar tides, which can supply upto half of the total energy input. Most of the remaining energy is believed to come from the winds, primarily in the Southern Ocean.

Although a vast amount of work is done by the winds on the ocean totaling some 20 TW, most of this remains in the surface layer and does not penetrate into the abyss where it would be available for deep ocean mixing.

The largest problem with energetic studies of the oceans is the lack of appropriate observations. The launch of satellite missions such as TOPEX/POSEIDON have provided a much greater coverage of the ocean surface, however observations in the ocean interior are still incredibly sparse, coming mainly from field campaigns which can only ever cover a tiny proportion of the ocean. This lack of observations causes the huge uncertainties in the oceanic energy budgets. Although it is possible to fill some of the gaps with model output, it is difficult to rely on this due to the lack of verification. It is also difficult to trust model results when conducting studies of energetics. This is due to the way that the stratification is maintained in general circulation models, which is usually done through the introduction of a universal, constant diapycnal upwelling. This upwelling has no energy source associated with it, and thus a potential energy source is introduced. As far as the author is aware, the magnitude of this spurious energy input has not been calculated. Given the accuracy with which energy budgets can be made, this is probably negligible on all but the longest model integrations, and may well continue to be even as the accuracy of energy budgets is improved. This energy input is of more concern to those who are interested in running ocean models under very different geological conditions. The universal upwelling is chosen to provide 'reasonable' agreement with available present day observations and may have to take a different value to do the same under different geological conditions.

Gnanadesikan (1999) proposed a two layer model of the thermohaline circulation, consisting of a well mixed surface layer and a stratified abyssal layer separated by the pycnocline. This model contained some of the key processes highlighted in the study of the energy budget of the oceans and was parameterized in terms of three of these processes. These were an Ekman upwelling of fluid in the Southern Ocean, driven by a zonal Southern Ocean wind stress, a sinking across the density gradient in the northern hemisphere and a diapycnal upwelling in the low latitudes. Given the energy arguments that have been discussed in this study it is undesirable to assume such a constant, independent diapyncal mixing rate. However, in such a simple 'one-dimensional' model there is no way

to parameterize diapycnal mixing any more accurately and so the introduction of potential energy into the circulation must be accepted. These processes were parameterized in terms of the depth of the pycnocline, resulting in a cubic equation. This model, though very simple, captures qualitatively, and to a certain degree quantitatively the behaviour of the thermohaline circulation. The upwelling in the Southern Ocean has a linear relationship to the wind stress and is insensitive to the depth of the pycnocline. However there is also a sinking term caused by an eddy return flow which increases linearly with pycnocline depth. The upwelling in the low latitudes is inversely proportional to the pycnocline depth, while the sinking in the northern hemisphere is proportional to its square. Due to the missing mixing problem, it was unclear what value of diapycnal diffusivity should be used in the model. The model was strongly dependent on diapycnal diffusivity so both the cases of implied and measured mixing were considered. Realistic overturning rates were only produced when the implied mixing rate of 10^{-4} m^2s^{-1} was used, the same value Munk estimated in 1966. This should not come as a suprise as the parameterization of low latitude upwelling, $Q_u = K_v A/D$, makes the same assumption of uniform upwelling and horizontal isopycnals that were made by Munk in his 1966 paper.

A wide variety of ocean models, from simple box to state of the art general circulation models have predicted the existence of two or more stable equilibria in the thermohaline circulation. One such possible equilibrium is where an increased freshwater transport eliminates or negates the density difference in the North Atlantic. While it has been established that the thermohaline circulation cannot be *driven* by this density difference, it is still *controlled* by it to a large degree, and such a change in the density gradient could cause any sinking in the northern latitudes to cease, confining any deep overturning circulation to between the low latitudes and Southern Ocean. In its present state, the thermohaline circulation transports a huge quantity of heat from equatorial regions to the North Atlantic and such a collapse of the circulation could have a drastic effect on the climate of the North Atlantic region, and possibly the whole of the northern hemisphere. Such scenarios are currently a highly active area of research.

The two layer model proposed by Gnanadesikan is unable to support multiple equilibria, as for all realistic values of the parameters only one physical solution of the model equation exists. In order to gain an understanding of the processes

behind multiple equilibria we turned to a two box model of the thermohaline circulation first proposed by Stömmel (1961). It was seen that salinity gradients caused by freshwater transport could cause a reversal in the circulation, which in this semi-hemispheric model caused a sinking in the low latitudes, which is probably an unphysical result due to the intense heating which occurs in tropical regions. This collapsed state existed for all non-negative values of freshwater transport, showing that once the circulation has collapsed there is no reason for it to revert to a northern sinking state if the climate is restored to its previous conditions.

Using the results from the Stömmel (1961) box model, an attempt was made to incorporate multiple equilibria into the Gnanadesikan (1999) two layer model. This was done by reparameterizing the northern sinking term into an implicit form whereby once the northern sinking weakened to a certain point it was effectively scaled down to zero, simulating the collapse of the circulation due a salt feedback. The threshold for this collapse was taken to be similar to that in the two box model at around 10 Sv. This scaling may lead one to believe that, unlike other models which exhibit multiple equilibria, the circulation would recover when whatever parameter was changed to cause the collapse is returned to its standard value. This did not happen, but rather two true, stable equilibria were found similar to those in the box model. In the collapsed state the pycnocline deepened significantly allowing fluid to be removed from the surface layer in the Southern Ocean, balancing that fluid upwelled in the low latitudes. The reason for the existance of the two true equilibria is the 'chicken and egg' situation created by the implicit parameterization of the northern hemisphere sinking term. Once the circulation has collapses, the only way for it to recover is for the northern sinking to increase past the critical value. This is reminiscent of the self-sustaining feedback mentioned in Chapter 4, where the circulation must carry enough salt north to allow fluid on the surface to become convectively unstable.

While the results obtained from the reparameterization of the northern sinking term were highly satisfactory, the reparameterization itself was not. It was included to account for haline feedback, but was completely ad hoc and had no rigorous physical basis. Any further work to be carried out on multiple equilibria in the Gnanadesikan two layer model should include an attempt to reparameterize the northern sinking term to include haline feedback on a more rigorous

physical basis, however it is difficult to see how this could be done without adding significant complication to what in its current state is a simple and elegant model.

Bibliography

[1] Alley, R.B., Marotzke, J., Nordhaus, W.D., Overpeck, J.T., Peteet, D.M., Pielke Jr., R.A., Pierrehumbert, R.T., Rhines, P.B., Stocker, T.F., Talley, L.D., Wallace, J.M. 2003. Abrupt Climate Change. *Science.* **299**:2005–2010

[2] Bennett, S.L. 1985. The Relationship between Vertical, Diapycnal, and Isopyncal Velocity and Mixing in the Ocean General Circulation. *J. Phys. Oceanogr.* **16**:167–174

[3] Bryan, F.O. 1987. Parameter sensitivity of primitive equation ocean general circulation models. *J. Phys. Oceanogr.* **17**:970–985

[4] Davis, R.E. 1994. Diapycnal Mixing in the Ocean: Equations for Large Scale Budgets. *J. Phys. Oceanogr.* **24**:777–800

[5] Davis, R.E. 1994. Diapycnal Minxing in the Ocean: The Osborn-Cox Model. *J. Phys. Oceanogr.* **24**:2560–2576

[6] Gill, A.E. 1982. Atmosphere-Ocean Dynamics. *Academic Press.*

[7] Gnanadesikan, A. 1999. A Simple Predictive Model for the Structure of the Oceanic Pycnocline. *Science.* **283**:2077–2079

[8] Hall, M.M., St. Laurent, L.C., Hogg, N.G. 2001. Abyssal Mixing in the Brazil Basin. *J. Phys. Oceanogr.* **31**:3331–3348

[9] Heywood, K.J., Garabato, A. C. N., Stevens, D. P. 2002. High Mixing Rates in the Abyssal Southern Ocean. *Nature.* **415**:1011–1014

[10] Huang, R.X. 1998. Mixing and Energetics of the Oceanic Thermohaline Circulation. *J. Phys. Oceanogr.* **29**:727–736

[11] Jeffreys, H. 1916. Causes Contributory to the Annual Variation of Latitude. *Mon. Not. R. Astron. Soc.* **76**:499–524

[12] Klinger, B.A., Drijfhout, S., Marotzke, J., Scott, J.R. 2003. Sensitivity of basin-wide meridional overturning to diapycnal diffusion and remote wind forcing in an idealized Atlantic-Southern Ocean geometry. *J. Phys. Oceanogr.* **33**:249–266

[13] Ledwell, J.R., Montgomery, E.T., Polzin, K.L., St. Laurent, L.C., Schmitt, R.W., Toole, J.M. 2000. Evidence for Enhanced Mixing Over Rough Topography in the Abyssal Ocean. *Nature.* **403**:79–182

[14] Lueck, R., Reid R. 1984. On the Production and Dissipation of Mechanical Energy in the Ocean. *J. Geophys. Res.* **89**:3439–3445

[15] Marotzke, J. 1997. Boundary Mixing and the Dynamics of Three-Dimensional Thermohaline Circulations. *J. Phys. Oceanogr.* **27**:1713–1728

[16] Marotzke, J., Willebrand, J. 1991. Multiple equilibria of the global thermohaline circulation. *J. Phys. Oceanogr.* **21**:1372–1385

[17] Marshall, D., 2005. Personal Communication.

[18] Munk, W., Wunsch, C. 1998. Abyssal Recipies II: Energetics of Tidal and Wind Mixing. *Deep-Sea Res.* **45**:1977–2010

[19] Munk, W.H. 1966. Abyssal Recipies. *Deep-Sea Res.* **13**:707–730

[20] Oort, A.H., Anderson, L.A., Peixoto, P. 1994. Estimates of the Energy Cycle of the Oceans. *J. Geophys. Res.* **99**:7665–7685

[21] Osborn, T.R. 1980. Estimates of the Local Rate of Vertical Diffusion from Dissipation Measurements. *J. Phys. Oceanogr.* **10**:83–89

[22] Paparella, F., Young, W.R. 2002. Horizontal Convection is Non-Turbulent. *J. Fluid. Mech.* **466**:205–214

[23] Rudnick, D.L., Boyd, T.J., Brinard, R.E., Carter, G.S., Egbert, G.D. 2003. From Tides to Mixing Along the Hawaiian Ridge. *Science.* **301**:355–357

[24] Sandström, J.W. 1908. Dynamicsche Versuche mit Meerwasser. *Annalen der Hydrographie under Martimen Meteorologie* **36**:6–23

[25] Scott, J.R., Marotzke, J., Adcroft, A. 2001. Geothermal Heating and its Influence on the Meridional Overturning Circulation. *J. Geophys. Res.* **106**:3141–3154

[26] Scott, J.R., Marotzke, J., Stone, P.H. 1999. Interhemispheric thermohaline circulation in a coupled box model. *J. Phys. Oceanogr.* **29**:351–365

[27] St. Laurent, L., Garrett, C. 2002. The Role of Internal Tides in Mixing the Deep Ocean. *J. Phys. Oceanogr.* **32**:2882–2899

[28] Stein, C.A., Stein, S. 1992. A Model for Global Variation in Oceanic Depth and Heat Flow with Lithospheric Age. *Nature.* **359**:123–129

[29] Stömmel, H. 1961. Thermohaline Convection with Two Stable Regimes of Flow. *Tellus.* **13**:131–126

[30] Toole, J.M., Polzin, K.L. Schmitt, R.W. 1994. Estimates of Diapycnal Mixing in the Abyssal Ocean. *Science.* **264**:1120–1123

[31] Toggweiler, J.R., Samuels, B. 1998. On the Ocean's Large Scale Circulation Near the Limit of No Vertical Mixing. *J. Phys. Oceanogr.* **28**:1832–1852

[32] Wunch, C., Ferrari, R. 2004. Vertical Mixing, Energy, and the General Circulation of the Oceans. *Annu. Rev. Fluid Mech.* **36**:281–314

[33] Wunsch, C. 1998. What is the Thermohaline Circulation? *Science.* **298**:1180–1181

[34] Wunsch, C., Stammer, D. 1997. Atmospheric Loading and the "Inverted Barometer" Effect. *Rev. Geophys.* **35**:79–107

[35] Wunsch. C. 1998. The Work Done by the Wind on the Oceanic General Circulation. *J. Phys. Oceanogr.* **28**:2332–2340